Environmental Pollution 255 (2019) 113166

Contents lists available at ScienceDirect

Environmental Pollution

journal homepage: www.elsevier.com/locate/envpol

Poly- and per-fluoroalkyl compounds in sediments of the Laurentian Great Lakes: Loadings, temporal trends, and sources determined by positive matrix factorization☆

Erik R. Christensen [a, *], Ruijie Zhang [b, c], Garry Codling [d], John P. Giesy [e, f], An Li [b]

[a] Department of Civil and Environmental Engineering, University of Wisconsin-Milwaukee, Milwaukee, WI 53201, USA
[b] School of Public Health, University of Illinois at Chicago, Chicago, IL 60612, USA
[c] School of Marine Sciences, Guangxi University, Nanning 530004, China
[d] Research Centre for Contaminants in the Environment, Pavilion 29, Masaryk University, Brno, Czech Republic
[e] Department of Veterinary Biomedical Sciences and Toxicology Centre, University of Saskatchewan, Saskatoon, SK S7N 5B3, Canada
[f] Department of Environmental Science, Baylor University, Waco, TX, United States

ARTICLE INFO

Article history:
Received 18 June 2019
Received in revised form
22 August 2019
Accepted 2 September 2019
Available online 14 September 2019

Keywords:
Poly- and per-fluorinated compounds
The Great Lakes
Sediment
Temporal trends
Positive matrix factorization

ABSTRACT

A recent data set for 22 poly- and per-fluorinated compounds (PFASs) in Ponar grab samples of surface sediments and cores from the Great Lakes of North America was examined for concentrations, loads, correlations with geographical coordinates and depth (time), and for sources. Correlations were determined by multivariate regression analyses. Source apportionment of PFASs was carried out by positive matrix factorization (PMF) for two cores from Lake Ontario. For the five lakes together, the total load of PFASs in sediments was estimated to be 245 ± 24 tonnes, which is about half the load for total PCBs. The recent annual loading was 1812 ± 320 kg/yr. Concentrations and inventories of PFASs were greatest in Lakes Erie and Ontario. Since 1947, concentrations of perfluorooctane sulfonic acid (PFOS) in ten cores have increased exponentially as a function of time with doubling times between 10 and 54 yr and have leveled off in three cores since 2000. PMF demonstrated an effective grouping of two particle-associated factors, characterized mainly by longer-chain PFASs ($C \geq 8$) and two other factors of mainly shorter-chain compounds ($C \leq 6$). Two factors feature only one dominant compound: factor 1, PFOS, and factor 3, perfluorobutane sulfonic acid (PFBS). Of all factors, factor 3 with PFBS has the largest contribution (47.8%). Significant scores for perfluorohexane sulfonic acid (PFHxS) and PFBS, along with flat or decreasing PFOS contributions since 2003, indicate that the replacement of PFOS with these compounds is beginning to take effect in the environment.

1. Introduction

Per- and poly-fluoroalkyl substances (PFASs) include carboxylic acids, sulfonic acids, and ethers that are fully or largely fluorinated, as well as their precursors and transformation products. PFASs have been and are still used in numerous consumer goods and have been found to be ubiquitous in the global environment (Prevedouros et al., 2006; Wang et al., 2013). Applications of PFASs include surface treatment of textile, leather, carpets, and food contact materials, metal plating, and fire-fighting foams. In 2002, the ubiquitous contamination of wildlife by perfluorooctane sulfonic acid (PFOS) was documented by Giesy and Kannan (2001), and in 2006 PFASs were detected across the Great Lakes (Giesy et al., 2006).

These and other studies led to global restrictions on production of longer chain PFASs. In the United States, under the toxic substances control act (TSCA), carboxylic acids with ≥8 carbons including perfluorooctanoic acid (PFOA), and sulfonates with >6 carbons including perfluorooctane sulfonic acid (PFOS) and perfluorohexane sulfonic acid (PFHxS) were phased out by 2015. Restrictions were applied by US EPA to PFOS in 2000 (US EPA, 2000) and to PFOA during 2010–2015 under the US EPA stewardship program, which was joined by eight international companies with business operations in the United States and other countries (US EPA, 2018a). Accordingly, in 2003, 3M replaced PFOS with perfluorobutanesulfonic acid (PFBS) in the consumer product

☆ This paper has been recommended for acceptance by Dr. Jörg Rinklebe.
* Corresponding author.
E-mail address: erc@uwm.edu (E.R. Christensen).

https://doi.org/10.1016/j.envpol.2019.113166
0269-7491/

Scotchgard and in 2009, DuPont (now Chemours) began production of GenX as a replacement for PFOA used in production of Teflon (Loughran and Mangahas, 2019; US EPA, 2018b). PFHxS has until recently been used as a substitute for PFOS, which was restricted under the Stockholm Convention in 2009, but has now been added to the candidate list of substances of very high concern (ECHA, 2019). Sources of PFASs include direct emissions as ingredient or impurities from the manufacturing and uses of host products. Indirect sources of PFASs include transformations of precursors in the environment and biota. For example, transformation of hydrofluorocarbons (HFCs) and hydrofluorethers (HFEs) to form perfluoroalkyl carboxylic acids (PFCAs) have been reported to occur in the atmosphere (Wang et al., 2014a).

PFASs are amphiphilic with combined hydrophilic and hydrophobic moieties in their molecules. The hydrophilic feature is due to their carboxylic or sulfonic "head" moieties, while their hydrophobic end is the $-CF_2-$ chain terminated by CF_3. Depending on the "head" and the length of the chain, the physicochemical properties vary. For the 22 individual PFASs studied, aqueous solubilities and octanol-water partition coefficients vary by orders of magnitude (US EPA, 2013). Compared with legacy persistent organic pollutants (POPs), most of which are hydrophobic, and resistant to degradation, knowledge about relatively hydrophilic POPs, including PFAS, is limited, presenting a challenge for understanding their transport and fate (Reemtsma et al., 2016). For example, profiles of concentrations of polar contaminants in undisturbed cores of sediments might deviate significantly from known production and use histories, thus cannot be used to describe temporal trends of releases. We have previously reported such challenges for organophosphate esters (Cao et al., 2017), atrazine and related herbicides (Guo et al., 2016), and shorter-chain PFASs (Codling et al., 2018a,b) in sediments of the Laurentian Great Lakes. New theories and tools are needed to retrieve the history and to predict future trends for chemicals that are relatively polar and thus mobile in natural waters.

Positive matrix factorization (PMF) is a factor analysis approach to achieve source apportionment of measured data. This is done by mathematically resolving a data matrix of measurements into a product of a loading matrix which contains source profiles, and a score matrix reflecting source contributions (Paatero, 1997). It has been demonstrated to be a useful tool in many applications. This includes analysis of source apportionment and dechlorination of polychlorinated biphenyls (PCBs) in sediment (Bzdusek et al., 2006; Praipipat et al., 2013), debromination of polybrominated diphenyl ethers (PBDEs) in sediment (Rodenburg et al., 2014; Zou et al., 2016), source apportionment of polychlorinated-*p*-dioxins and polychlorinated dibenzofurans (PCDD/F) in sediment (Sundqvist et al., 2010), and characterization of volatile organic compounds (VOCs) from vehicular emissions (Li et al., 2017). However, to our knowledge, it has not been used previously for evaluating sources and possible partitioning behavior of PFASs.

The objective of this study was to provide insight into post-depositional behavior of PFAS in sediment of the Great Lakes. To describe temporal trends more accurately, concentrations of PFASs were converted to fluxes and inventories were estimated for individual sampling sites. We also provide, for the first time, lake- and region-wide estimates for total accumulation and annual input to sediments of the Great Lakes and present the region-wide spatial distribution of concentrations and loadings. Additionally, we applied equilibrium partitioning theory to examine extents of sorption and downward movement of PFASs in sediment. We also evaluated feasibility of using a PMF model to identify common behaviors of PFASs, examined validity of the historical record, and obtained information about sources.

2. Materials and methods

2.1. The data set

Samples of sediments used in this study were collected from 2010 to 2015 as part of a Great Lakes sediment surveillance program. A total of 1137 samples were collected, including 198 Ponar grabs and 939 core segments from 40 cores. The sampling locations are shown in Fig. S1 of Appendix A, and more detailed description can be found in Li et al. (2018). Dry and wet bulk densities, particle content, and the fractions of organic carbon, organic matter, black carbon, and total nitrogen were determined for all samples of sediments (Bonina et al., 2018; Hosseini, 2016). All sections of cores were dated by use of multiple radioactive isotopes (Corcoran et al., 2018). Twenty-two PFASs listed in Table 1 were quantified. These include 16 perfluroalkyl compounds and 6 perfluorinated precursors. Branched isomers of PFASs were also produced during manufacture but were not included in this project. Identification and quantification of target PFASs were done by high-performance liquid chromatography (HPLC) coupled with triple quadruple mass spectrometry (MS/MS). Quality control included limit of quantification; instrument detection limit; field, travel, and solvent blanks; and internal standard and surrogate recoveries. Extractable organic fluorine was measured by combustion ion chromatography. All measured concentrations of PFASs and fluorine have been previously reported (Codling et al., 2014, 2018a,b).

2.2. Annual and total loadings

The data for sediment cores were used to estimate segment-specific, apparent net deposition flux (Equation (1)) and the site-specific inventory (Equation (2)). The net flux is a scalar quantity presenting the rate of accumulation or loss per unit area per year at the site (Li et al., 2018). The inventory is an estimate of the total accumulation over the depth of sediment core per unit area of the lake bottom at sites. Then, the lake-wide parameters, apparent annual loading rate (Equation (3)) and total loadings (Equation (4)), were derived from the mean net flux and mean inventory, respectively, for individual lakes.

$$\text{Apparent net deposition flux}\left(\text{ng cm}^{-2}\text{ y}^{-1}\right) = c_i \times \text{MSR} / \text{FF} \quad (1)$$

$$\text{Inventory}\left(\text{ng cm}^{-2}\right) = \sum c_i\, \rho_{b,i}\, d_i \quad (2)$$

$$\text{Apparent annual loading rate}\left(\text{tonnes y}^{-1}\right) = \text{mean flux} \times \text{Lake water surface area} \times 10^{-5} \quad (3)$$

$$\text{Total load}\left(\text{tonnes}\right) = \text{mean inventory} \times \text{Lake water surface area} \times 10^{-5} \quad (4)$$

where c_i is the concentration, $\rho_{b,i}$ is the dry mass bulk density (g cm^{-3}) and d_i is the thickness (cm) of segment i. The recent annual loading is derived from Equation (1) with $i = 1$. The mass sedimentation rate MSR is in g cm^{-2} y^{-1} and the focusing factor FF is dimensionless. The focusing factor was estimated based on ^{210}Pb inventories (Corcoran et al., 2018). Water surface areas of Lakes Superior, Michigan, Huron, Erie, and Ontario are 82,100, 57,800, 59,600, 25,700, and 18,960 km^2, respectively. Other constants are for conversions of units. A similar approach was used for legacy polychlorinated POPs (Li et al., 2018).

Table 1
Estimated lake-wide recent total loads (tonnes) of individual PFASs in sediments of the Great Lakes.

Abbreviation	Compound	Superior	Michigan	Huron	Erie	Ontario	All Lakes
Perfluoroalkyl compounds							
PFBA	Perfluoro-n-butanoic acid	4.37	0.74	3.30	10.84	8.91	28.17
PFPeA	Perfluoro-n-pentanoic acid	1.84	0.22	0.52	4.80	0.33	7.70
PFHxA	Perfluoro-n-hexanoic acid	1.10	0.27	0.76	4.13	5.15	11.42
PFHpA	Perfluoro-n-heptanoic acid	2.17	1.99	0.23	0.71	0.20	5.30
PFOA	Perfluoro-n-octanoic acid	1.10	0.85	0.70	2.53	2.68	7.86
PFNA	Perfluoro-n-nonanoic acid	2.12	0.51	0.31	2.30	6.58	11.81
PFDA	Perfluoro-n-decanoic acid	12.46	1.73	0.04	15.14	1.89	31.25
PFUnDA	Perfluoro-n-undecanoic acid	0.77	0.26	0.66	39.01	6.60	47.30
PFDoDA	Perfluoro-n-dodecanoic acid	0.00	0.16	0.12	0.01	0.17	0.46
PFTrDA	Perfluoro-n-tridecanoic acid	0.48	0.31	0.16	0.33	2.89	4.18
PFTeDA	Perfluoro-n-tetradecanoic acid	0.95	0.59	0.11	0.13	1.97	3.76
PFHxDA	Perfluoro-n-hexadecanoic acid	0.13	0.04	0.37	0.15	0.65	1.33
PFBS	Perfluoro-1-butanesulfonate	1.20	2.06	0.42	17.50	17.11	38.29
PFHxS	Perfluoro-1-hexanesulfonate	0.39	1.83	0.27	3.54	1.85	7.87
PFOS	Perfluoro-1-octanesulfonate	0.28	3.72	1.55	4.34	4.90	14.80
PFDS	Perfluoro-1-decanesulfonate	0.44	1.29	0.04	11.93	2.62	16.32
Perfluorinated precursors							
FOSA	Perfluoro-1-octanesulfonamide	0.02	0.01	0.12	0.83	0.01	0.87
FOSAA	Perfluoro-1-octanesulfonamidoacetic acid	0.04	0.25	0.12	0.07	0.12	0.61
N-MeFOSAA	N-methylperfluoro-1-octanesulfonamidoacetic acid	0.24	0.85	[a]na	0.62	0.01	1.71
NEtFOSAA	N-ethylperfluoro-1-octanesulfonamidoacetic acid	0.22	1.09	na	0.07	0.74	2.12
NMeFOSE	2-N-methylperfluoro-1-octanesulfonamidoethanol	[b]0	1.05	na	na	na	1.05
NEtFOSE	2-N-ethylperfluoro-1-octanesulfonamidoethanol	0	1.09	na	na	na	1.09
∑PFASs		30.3 ± 5.1	20.9 ± 2.3	9.90 ± 3.1	119 ± 21.2	65.4 ± 8.0	245 ± 24

[a] na = not analyzed.
[b] 0 = not detected.

2.3. Correlations

The chronological trends of the concentrations of PFASs to the Great Lakes sediment show a general pattern of increase with time (Codling et al., 2018a, 2018b). Based on these observations, net fluxes to sediments were calculated. These net fluxes integrated all input and potential output processes to each segment of cores and incorporated effects of sedimentation rate and sediment focusing. Linear regressions with one independent variable, year, and one dependent variable, Ln net flux of PFOS, were developed by use of the Analysis Toolpak in MS Excel. Doubling times, t_2, of net fluxes were calculated as ln 2 divided by the slope of the log-linear regression.

Linear regressions with two independent variables, latitude and longitude of the sampling sites, and one dependent variable, either Ln $\sum_{22}$PFAS concentrations in Ponar grab samples or Ln$\sum_{22}$PFAS inventories at coring sites, were used to develop geographical correlations using a multivariate regression function in Excel. Such correlations could be expected due to increased PFAS pollution at lower latitudes near urbanized areas moving south, and increased PFAS pollution at lower absolute longitudes moving east towards industrial activity around Lakes Erie and Ontario (Fig. 1). The methodology is an extension of the approach using a single independent variable (either latitude or longitude) for PCBs (Li et al., 2009) or flame retardants (Yang et al., 2012) into plotting them as a function of a linear sum of latitude and longitude.

2.4. PMF modeling

Positive matrix factorization (Zou et al., 2016; Paatero and Tapper, 1994; Paatero, 1997; Bzdusek, 2005) was used to resolve data matrices **X** (m x n) for PFASs, where m = number of compounds and n = number of samples, into products of a loading or source profile matrix **G**(m x f) where f = number of factors and a score or contribution matrix **F**(f x n),

$$X = G\,F + E \tag{5}$$

where **E** (m x n) is an error matrix. The data matrix **X** contains m rows of each of n PFAS concentrations. Prior to PMF analysis, concentrations for each sample in the data matrix **X** were scaled by dividing by the mean concentration for each sample. When analyses were completed, PFAS loadings (source profiles) in matrix **G** were back scaled by multiplying by mean concentrations. Each element of the **G** matrix becomes the fraction of compound j in factor k, such that the sum of column values of the **G** matrix is unity or 100%. Factor contributions (%) were calculated as the sum of all matrix elements of a row in the **F** matrix, for each factor, over the aggregate sum for all factors. The PMF Matlab code listed in the PhD thesis by Bzdusek (2005), and further described elsewhere (Bzdusek et al., 2006) was used for all PMF calculations. The relative error for the weighting function was set to 0.2. Further discussion of the PMF model is provided in Supporting Information, Appendix A.

2.5. PFASs in pore water from K_{oc} calculations

Association of PFASs with particles is characterized by their fractions dissolved in pore water of the sediment. Under the assumption of equilibrium partitioning between PFASs in pore water and sediment organic carbon, the fraction in interstitial water or pore water of PFASs, f_{iw}, can be determined using Equation (6) (Cao et al., 2017):

$$f_{iw} = \frac{1}{1 + r_{sw} \cdot K_{oc} \cdot f_{oc}} \tag{6}$$

where K_{oc} is the organic carbon partition coefficient, f_{oc} is the organic carbon fraction, and r_{sw} is the solid-to-water mass ratio which equals sediment dry bulk density divided by porosity. Dry bulk density and porosity were measured, and the organic carbon partition coefficient was determined from the US EPA Estimation Program Interface Suite using the K_{ow} method (US EPA, 2013). For a

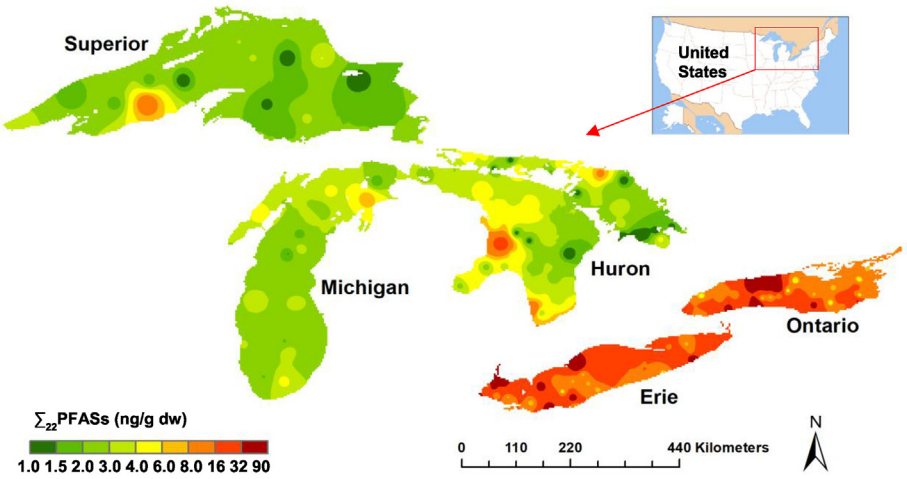

Fig. 1. Spatial distribution of the concentrations of Σ_{22}PFASs in Ponar grab samples, illustrated using the inverse distance weight (IDW) interpretation in the geostatistical analysis tool of ArcGIS 10.3 (Redlands, CA).

given PMF factor, the overall pore water fraction was calculated by adding contributions from each PFAS of the factor considered.

3. Results and discussion

3.1. Spatial distribution and annual and total loadings

Spatial distributions of the summed concentrations of 22 PFASs, $\sum_{22}$PFASs, in Ponar grab sediments is illustrated in Fig. 1 using the inverse distance weight (IDW) interpolation in the geostatistical analysis ArcGIS (Redlands, CA). The $\sum_{22}$PFASs in this figure included data that were less than the limit of detection DL, and they were summed as DL/2. Most $\sum_{22}$PFASs vary from lesser concentrations (1–3 ng/g dw) in Lake Superior, to intermediate concentrations (1–6 ng/g dw) in Lakes Michigan and Huron, and greater concentrations (8–90 ng/g dw) in Lakes Erie and Ontario. Concentrations are shown in a column diagram in Fig. S2. Potential sources of emissions of PFASs in the Great Lakes region have been discussed previously (Codling et al., 2018a,b, 2014). The top three hot spots found in this work are listed in Table S1. Locally elevated contamination is seen near airports, industries, and wastewater treatment plants. Inventories of $\sum_{22}$PFASs were greater near the mouth of the Detroit River (ER92), the mouth of the Niagara River (ON02, ON06), and by Wolfe Island near the outlet of Lake Ontario (ON36). ER92 is the only core taken from the western basin of Lake Erie, and it might accumulate contaminants released from the industrialized city of Detroit. ON06 has been found to have the largest inventories for various major legacy and emerging pollutants including PCBs, PCDFs, PCNs, and PCDEs (Li et al., 2018).

The amount of extractable organic fluorine (EOF) was between 2 and 44% of the fluorine in known PFASs in surface sediment from Lake Ontario. The unidentified organic fluorine could potentially degrade to persistent perfluorocarboxylates and perfluoroalkane sulfonates (Yeung et al., 2013). Codling et al. (2018b) found that EOF was 2–3 orders of magnitude greater in Lakes Erie and Ontario than were concentrations of PFAS.

Total loads of $\sum_{22}$PFASs are summarized in Table 1 and annual loadings in Appendix A, Table S2. Total accumulation of ΣPFASs in the Great Lakes sediment equates to 245 ± 24 tonnes. This is between 1.1 and 9.4% of the total global emissions of PFCAs, a subgroup of PFASs, from 1951 to 2015 (Wang et al., 2014b). For the Great Lakes it is about half of the total load for PCBs, but much greater than the loads of other important legacy polychlorinated pollutant groups (Li et al., 2018) as well as PBDEs (Li et al., 2006) and other flame-retardant groups of emerging concern (Yang et al., 2012, 2011). Total loads were maximal in Lakes Erie and Ontario with values of 119 ± 21.2 and 65.4 ± 8.0 tonnes, respectively, which indicated industrial and wastewater sources (Codling et al., 2018b). Recent annual loadings were calculated as 1812 ± 320 kg/yr, which is between 0.43 and 2.4% of the recent total global annual emissions of PFCAs (Wang et al., 2014b). Recent annual loadings were also greater in Lakes Erie (809 ± 282 kg/yr) and Ontario (684 ± 282 kg/yr) than in the other three lakes. Uncertainties or standard deviations are calculated as follows. For example, for Lake Ontario the uncertainty is (Equation (7)),

$$\delta_O = \sqrt{\sum_i \delta_i^2} \tag{7}$$

where δ_i = standard deviation of mean load or loading for each PFAS *i*. The standard deviation of the total load is calculated as the square root of the sum of uncertainties of loads squared for all five lakes (Equation (8)),

$$\delta = \sqrt{\delta_S^2 + \delta_M^2 + \delta_H^2 + \delta_E^2 + \delta_O^2} \tag{8}$$

where the subscripts refer to Lakes Superior (S), Michigan (M), Huron (H), Erie (E), and Ontario (O). Relative uncertainties are greater for recent annual loadings than for total loads because recent annual loadings depend on concentrations of PFASs in the uppermost sediment layer which can be quite variable, and even zero, as for example for cores S001 which was not datable, and S002, which had concentrations below instrumental detection limits.

3.2. Correlations of PFASs with geographical coordinates

Multivariate linear regression equations were obtained for the natural logarithm of concentrations in Ponar grab samples, before and after normalization by sediment organic carbon (OC) content, with independent variables latitude and longitude of the sampling sites (Equations (9) and (10)).

$$\text{Ln} \sum 22\text{PFASs conc.} \left(\text{ng/g dw}\right) = 26.78 \left(\pm 2.02\right) + \text{a x Latitude} + \text{b x Longitude} \quad (9)$$

$$\text{Ln} \sum 22\text{PFASs conc.} \left(\text{ng/g OC}\right) = 24.97 \left(\pm 2.86\right) + \text{a x Latitude} + \text{b x Longitude} \quad (10)$$

where dw = dry weight; a = - 0.315 ± 0.046 and b = 0.137 ± 0.023, $R^2 = 0.489$ in Equation (9); and a = - 0.192 ± 0.065 and b = 0.128 ± 0.033, $R^2 = 0.217$ in Equation (10). A similar regression was performed with core inventory as the dependent variable (Equation (11)).

$$\text{Ln} \sum 22\text{PFASs 1nv.} \left(\text{ng/cm}^2\right) = 24.65 \left(\pm 4.95\right) + \text{a x Latitude} + \text{b x Longitude} \quad (11)$$

where a = - 0.153 ± 0.120 and b = 0.166 ± 0.057, $R^2 = 0.343$.

Additional statistical parameters are listed in Table S3. Plots of measured vs. calculated values are shown in Fig. S3. Meanings of a and b, in Equation (9), are contributions to the log function from latitude (−0.315/deg latitude) or longitude (0.137/deg longitude) (Table S3). As is the case for many other POPs, concentrations and inventories of PFASs in sediments tend to be greater at lower latitudes and lower absolute longitudes over the entire region. Such a trend is expected because of increasing urbanization towards south and denser local sources of PFASs, including chemical industries, towards the east. Calculated values for Lakes Erie and Ontario were similar because of the lower latitude but higher absolute value of longitude of Lake Erie relative to Lake Ontario. The inventory for Lake Huron was least among the five lakes (Fig. S2B), which is consistent with its least total load of 9.90 ± 3.1 tonnes (Table 1). The coefficient of determination (R^2) of 0.49 for concentrations (Equation (9)) indicates that the latitude and longitude together explain 49% of variations in concentrations of $\sum_{22}$PFASs in sediment. Using only latitude and longitude as independent variables would work best in the cases when all locations receive the chemical from similar and consistent sources, for example, atmosphere deposition. The results from our correlation analyses suggest the impacts of local discharges and complements the map (Fig. 1) of the spatial distribution of PFASs in the Great Lakes sediment.

Normalization of concentrations of PFASs to OC (%) did not improve correlations with latitude and longitude. This is different from more legacy and/or hydrophobic organic contaminants such as PCBs (Li et al., 2009), PBDEs (Li et al., 2006), and chlorinated flame retardants (Yang et al., 2011), where concentrations normalized to OC or organic matter content tend to strengthen correlations with latitude and/or longitude. The coefficient of determination R^2 was 0.217 with normalization to OC and 0.489 without it (Table S3). Restricting the correlation to 96 Ponar samples within depositional sub basins with $\rho_b \leq 0.45$ g/cm^3, produces a moderately higher $R^2 = 0.290$ (Table S3). Note that there is an increase in $\sum_{22}$PFASs concentration with OC values below about 20 mg/g, especially for lakes Superior, Michigan, and Huron as well as the North Channel and Georgian Bay, but no further increase at OC > 20 mg/g for Lakes Erie and Ontario (Fig. S4). This indicates that hydrophobic carbon association is not the only sorption mechanism, but that other effects such as pH and electrostatic interactions play a role (Higgins and Luthy, 2006).

For emerging pollutants such as PFASs, proximity to localized sources can outweigh any sediment characteristics in determining the spatial distribution pattern of their concentrations in environmental matrices. An example of this is the apparent outlier station S119 in Lake Superior (Figs. S1, S2, S4) near the town of Ontonagon, Michigan which might be influenced by PFASs from the former Smurfit-Stone Container paper mill (Codling et al., 2018a). Another example is site H108, which is close to the Wurtsmith Air Force Base and had the greatest $\sum_{22}$PFASs concentration (26.0 ng/g) in Lake Huron at OC = 2.99 mg/g (Figs. S1, S2, S4). Site H108 is in a non-depositional area with dry bulk density $\rho_b = 1.09$ g/cm^3.

3.3. Temporal trends and downward mobility

Net fluxes versus year of deposition in core segments dated to have been deposited in 1940 or later were best described by first-order kinetics for PFOS at selected sites in Lakes Michigan and Ontario (Fig. 2 and Table S4). For PFOS, when excluding regressions with negative slopes and statistically insignificant values, apparent doubling times t_2 ranged from 10 to 54 yr with a mean of 24 yr. The mostly satisfactory fits of log-linear regressions suggest nearly exponential increases in loadings of PFOS after 1940 until the phase-out in 2000. The actual doubling time of input to the lakes could be shorter than these apparent t_2 values derived from sediment data, given the possible post-depositional downward diffusion within sediment over time, even for a relatively hydrophobic PFAS, such as PFOS. The outlier with the longest doubling time is

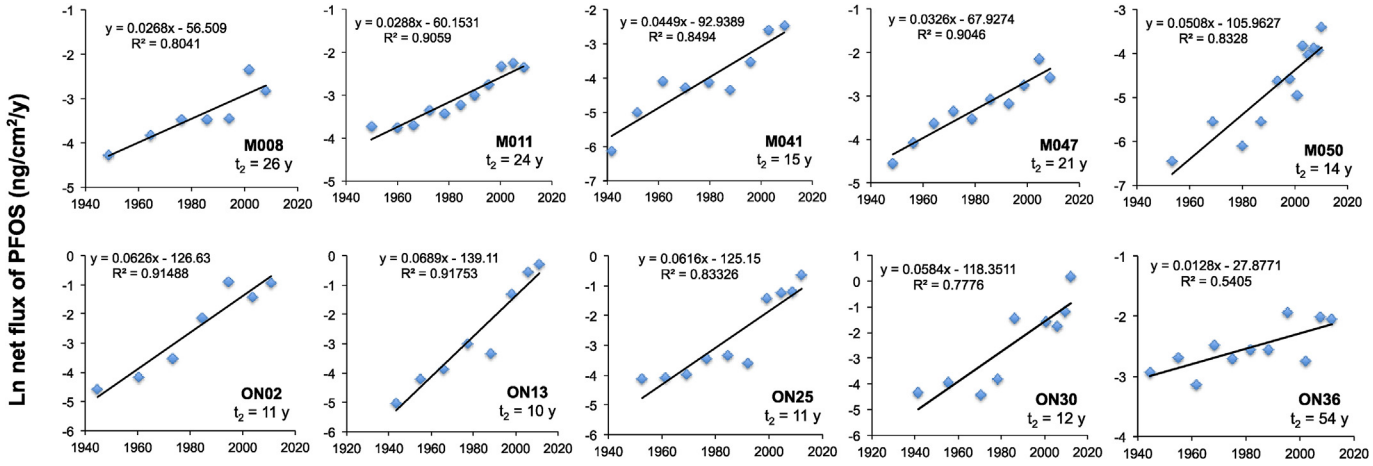

Fig. 2. First-order kinetic plots of net flux of PFOS to sediment at selected core sampling sites in Lakes Michigan and Ontario. The apparent doubling time in years was calculated using $t_2 = \ln(2)/\text{slope}$. All the regressions shown are significant at $p < 0.05$ (see Table S4).

ON36 ($t_2 = 54$ yr). From Fig. S2 it is apparent that location is important for determining concentrations of PFASs. Considering that ON36 is well dated and that PFOS is associated with particulates and follows the expected dating through factor 1 (Figs. 3 and 4), the likely main reason for the longer doubling time for ON36 is that a local source near Wolfe Island might be characterized by a relatively slow PFAS increase vs time. Myers et al. (2012) found increasing concentrations of PFOS, PFOA, PFDS, FOSA, PFHpA, PFNA, and PFUnDA vs time, starting between 1942 and 1980, in three basins of Lake Ontario; but no doubling times were derived and reported. In this work, we noticed that at a few sites, i.e. M011, ON02, ON36, the net flux of PFOS shows a flattening after year 2000. This is in accordance with the finding of Yeung et al. (2013) who, by investigating a core from mid-Lake Ontario, observed increasing concentrations of PFOS and PFBA vs time with leveling off around year 2000. We believe that such flattening trends are an indication that the restrictions on PFOS production and usage since the early 2000s have been effective.

An indication of hydrophobicity of PFOS compared to shorter-chain ($C \leq 6$) PFASs, such as PFHxA and PFBS, can be seen from net fluxes of all three compounds vs year in cores from Lake Superior, Michigan, Huron, and Ontario (Fig. S5). Lake Erie is not

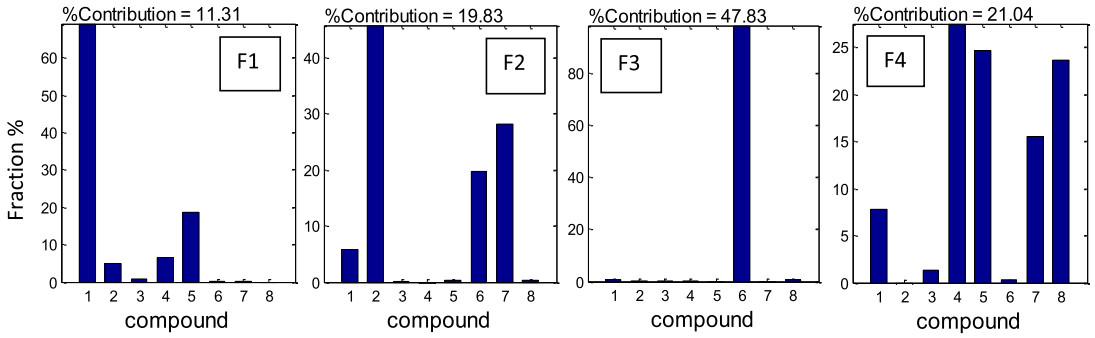

	Compound	Coefficient of Determination
1	PFOS	0.674
2	PFHxA	0.781
3	PFHpA	0.650
4	PFNA	0.806
5	PFDA	0.796
6	PFBS	0.943
7	PFHxS	0.710
8	PFTrDA	0.836

Fig. 3. Loading of PFASs for each of four PMF factors F1, F2, F3, and F4 for Lake Ontario cores ON02 and ON36.

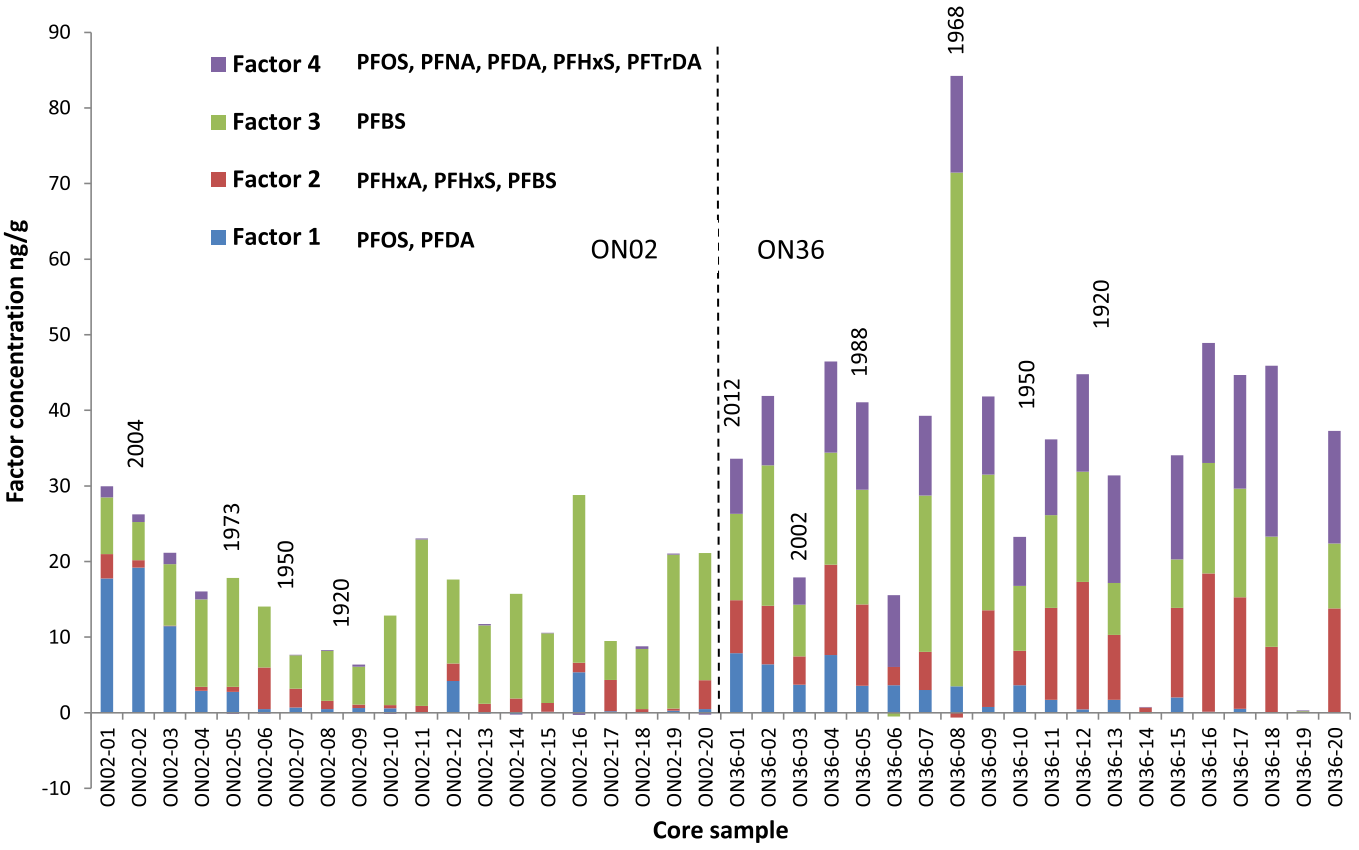

Fig. 4. Factor score map for Lake Ontario cores ON02 and ON36. Dates are determined from the CRS model (Corcoran et al., 2018).

included due to significant sediment mixing (Corcoran et al., 2018; Fisher et al., 1980). Fluxes of PFOS in Lake Superior core S011 and Lake Michigan core M009 were virtually zero before 1947, when PFOS production started, whereas PFHxA and PFBS exhibited significant net fluxes before 1947 (Fig. S5). This observation suggested presence of PFHxA and PFBS in pore water and downward movement within sediment, as these shorter PFASs were not manufactured before the 1950s (US EPA, 2018c). This is approximately true also for cores H006 in Lake Huron and core ON36 in Lake Ontario.

3.4. PMF modeling of PFASs

As outlined in Appendix A, cores ON2 and ON36 from Lake Ontario were selected for analysis based on criteria for a valid PMF solution and few numbers of non-detects. There were 320 data points in the matrix for PFOS, PFHxA, PFHpA, PFNA, PFDA, PFBS, PFHxS, and PFTrDA in cores ON02 and ON36 (Table S5) and 87% of these concentrations were greater than limit of detection. The Exner value was 0.0774 ($R^2 = 0.774$), and the coefficients of determination for individual PFASs between 0.650 and 0.943 (Fig. 3) which supports the results of the PMF analysis. The number of factors was found to be four: factors 1 (PFOS, PFDA) and 4 (PFOS, PFNA, PFDA, PFHxS, PFTrDA) represent mostly longer-chain ($C > 8$) PFASs, whereas factors 2 (PFHxA, PFHxS, PFBS) and 3 (PFBS) reflect shorter-chain ($C = 4–6$) PFASs (Figs. 3 and 4).

Factor 1 is dominated by PFOS and PFDA (Fig. 3). These compounds are known to bind to sediment (Zhao et al., 2012; Zushi et al., 2010). Its temporal profiles (Fig. 4) largely matched the history of production which started in the 1940s. The maximum Factor 1 in ON02 occurs near 2004, about the time (2003) when 3M replaced PFOS with PFBS in the consumer product Scotchgard. Consistent with our observation, maximum concentrations of PFOS were observed near 2005 in sediment cores from Tokyo Bay, Japan (Ahrens et al., 2009). PFOS largely diminished in deeper core segments at most coring locations (Figs. 2 and 4).

Factor 2 contains medium chain length C4–C6 PFASs which are dispersed throughout the cores from both sites ON02 and ON36 (Fig. 4), reflecting their significant presence in porewater due to high water solubilities: PFHxA 15,700 mg/L, PFBS 344 mg/L, and PFHxS 6.2 mg/L at 25 °C. Both PFHxS and PFBS are replacement products for PFOS which was restricted under the Stockholm convention on persistent organic pollutants (POPs) in May 2009. PFHxS might be present in fire-fighting foams and is along with PFHxA used for making household products stain resistant and making clothes more waterproof.

Factor 3 representing only PFBS has a major presence, especially in core ON02, and is seen throughout both cores ON02 and ON36 due to its significant water solubility and resulting vertical mobility. In Lake Ontario, PFBS is the most abundant among all 22 PFASs analyzed in this work (Table 1).

Factor 4 including mostly long chain C6–C13 compounds has a small presence and near historical record in core ON02 with increased concentration in the top four layers since 1985. A similar pattern was reported for PFUdA ($C_{11}HF_{21}O_2$) in units of ng/g dw or ng/g OC in top layers of cores from Tokyo Bay (Ahrens et al., 2009; Zushi et al., 2010). The latter authors found a similar trend for PFTrDA expressed in units of ng/g OC, while factor 4 is widely dispersed in core ON36 probably due to higher temperature (Bečanová et al., 2016) and higher pH (Higgins and Luthy, 2006) which might result in greater concentrations of PFASs in porewater and therefore greater post-depositional diffusion.

Due to hydrophobic interactions, OC in sediments tends to enhance the sorption of PFASs to sediment (Bečanová et al., 2016; Higgins and Luthy, 2006). This is also the case for the Great Lakes where the sum of PFASs increases with organic carbon at $OC < 20$ mg/g for Lake Superior, Michigan, and Huron and the North Channel and Georgian Bay (Fig. S4). However, correlations between OC in sediments of Nansi Lake in China and sediment-water partition coefficients (K_d) for PFASs were small (Cao et al., 2015). Core ON02, which was located near the Niagara River outlet in the western part of Lake Ontario, with a water depth of 101 m and OC content between 49 and 15 mg/g, could be influenced by Niagara River and atmospheric input, whereas core ON36, near the mouth of the St. Lawrence River and with a water depth of 26 m and OC content between 71 and 27 mg/g, might have received significant input to the water phase from local sources.

Considering all four factors, for both cores ON02 and ON36, there are peaks near 1970, in 1973 and 1968 for cores ON02 and ON36, respectively (Fig. 4). It appears that following the Clean Water Act 1972, there was a general reduction in pollution input. However, there was a rapid increase in net input flux of PFOS after 1990 with a maximum around 2005, especially in core ON02. This indicates an input commensurate with the maximum global production of 4500 t/yr (Codling et al., 2018a).

3.5. Partitioning of PFASs in the sediment

Further support for the validity of the PMF factors might be obtained from a calculation of the interstitial water fraction f_{iw} for PFASs in each factor following Equation (6). For example, factor 1 featuring the long-chain C8–C10 PFOS and PFDA, that are known to bind to sediment, would be expected to have a low f_{iw}, while factor 3, displaying only the more hydrophilic short chain C4 PFBS is expected to have a high f_{iw}. Calculated values of log K_{oc} along with pKa are shown in Table S6.

Two types of analysis support the log K_{oc} numbers listed in Table S6. The first illustrates that Log K_{oc} values for different compounds relate to one another following rules for Log K_{oc} for PFASs applied by Higgins and Luthy (2006). The other approach is to compare with field determined Log K_{oc} values as shown below. According to Higgins and Luthy (2006), a sediment parameter that can influence partitioning between water and sediment for linear PFAS isomers is length of the carbon chain in perfluorocarbon. Each CF_2 moiety contributes 0.50–0.60 log units to the distribution coefficient and the sulfonate moiety generally contributes an additional 0.23 log units to the distribution coefficient compared with analog carboxylate compounds. Thus, from $\log K_{oc} = 2.45$ for PFHpA (Table S6) we would expect $\log K_{oc} = 2.45 + 0.23 = 2.68$ for PFHxS which is near the value listed in Table S6 (2.67). Also, when log K_{oc} for PFHxA is estimated from PFHxS and PFHpA, $\log K_{oc} = 2.67–0.23 - 0.4 = 2.04$ were obtained, which is near 2.08 (Table S6). This calculation was calculated based on 0.4 log units for the contributions of CF_2 moieties. The greater log K_{oc} of PFHxS compared to PFHxA, both containing six carbon atoms, is consistent with the composition of factors 2 and 4. Factor 2, representing partially soluble PFASs, has a greater fraction of PFHxA than of PFHxS, and factor 4, reflecting particle associated compounds, has a significant fraction of PFHxS but not PFHxA.

Calculated log K_{oc} values used in this study (Table S6) are comparable to values of 2.97 ± 0.03, 1.75 ± 0.01, and 3.23 ± 0.07 for PFOS, PFBS, and PFDA, respectively, measured in a bulk sediment from the Haihe River, China (Zhao et al., 2012). With pKa <1 and at ambient pH, the log K_{oc} values in Table S6 reflect fully ionized compounds. Calculated pore water fraction for PFAS in layers of cores ON02 and ON36 are shown in Tables S7 and S8, and for each PMF factor in Fig. S6. All pore water fractions for factors 1 and 4 containing longer-chain PFASs were less than 10%, confirming their likely association with particles in sediments. By contrast, factors 2 and 3 containing C4 – C6 compounds exhibited significant

proportions in pore water, between 30% and 60%. This supports the validity of the PMF method to group PFASs according to their tendency to bind to sediment. Based on this work, PFASs that sorb more tightly to sediment include PFOS and PFDA, while PFHxS and PFBS exhibit intermediate or minor affinities. Similar findings in different settings were reached by Zhao et al. (2012) and Cao et al. (2015). The present work suggests that PFHxA has a major presence in pore water.

4. Conclusions

This report is the first to present PFAS loadings to sediments of the Great Lakes; to investigate dated sediment records of PFOS analyzed by first-order kinetics for several stations in Lake Michigan and Lake Ontario; and to evaluate dated records of PFOS vs PFHxA and PFBS for Lakes Superior, Michigan, and Huron. It is also the first to present PMF source apportionment of sediment PFASs for any water body. Dating of ten cores from Lakes Michigan and Ontario shows a nearly exponential increase of PFOS since 1947 with flattening in three cores since 2000. While dated records in undisturbed cores show little PFOS before 1947, there is evidence of PFHxA and PFBS before this time attesting to the vertical transport in porewater of these compounds. PMF analysis of the Lake Ontario PFASs data provides a useful grouping of PFASs with related properties. Factor 1 represents PFOS and PFDA bound to particles that are consistent with historical input records, factors 2 and 3 include PFASs of chain length <7 carbon atoms that have significant fractions in porewater, especially for core ON36, and factor 4 represents longer-chain carboxylic PFASs (PFOS, PFNA, PFDA, and PFTrDA) and minor fractions of PFHxS with nearly historical record in core ON02 and extensive porewater contribution in core ON36. The present work confirms previous findings that PFOS and PFDA bind tightly to sediments, and it also demonstrates that this might also apply to longer-chain PFASs PFNA, and PFTrDA, and possibly PFHxS. Factor 2 is dominated by PFHxA. The major contribution (47.8%) of factor 3, dominated by only PFBS, which also has a significant presence in factor 2, points to a common unique source of PFBS, probably related to the replacement of PFOS (C8) with the shorter chain and less toxic PFBS (C4).

Conflicts of interest

None of the five authors have any conflict of interest in the contents of this paper.

Acknowledgements

The data used in this research were obtained during the Great Lakes Sediment Surveillance Program, which was funded by a Cooperative Agreement from the US EPA Great Lakes Restoration Initiative with Assistance No. GL-00E00538 (EPA Program Officers Todd Nettesheim and Elizabeth Murphy). Matching funds have been provided by the University of Saskatchewan. JPG was supported by the Canada Research Chairs Program of the Natural Sciences and Engineering Research Council of Canada, and G. Codling by Masaryk University through the CETOCOEN PLUS (CZ.02.1.01/0.0/0.0/15_003/0000469) project and the RECETOX Research Infrastructure (LM2015051).

Appendix A. Supplementary data

Supplementary data to this article can be found online at https://doi.org/10.1016/j.envpol.2019.113166.

References

Ahrens, L., Yamashita, N., Yeung, L.W.Y., Taniyasu, S., Horii, Y., Lam, P.K.S., Ebinghaus, R., 2009. Partitioning behavior of per- and polyfluoroalkyl compounds between pore water and sediment in two sediment cores from Tokyo Bay, Japan. Environ. Sci. Technol. 43, 6969–6975.

Bečanová, J., Komprdová, K., Vrana, B., Klánová, J., 2016. Annual dynamics of perfluorinated compounds in sediment: a case study in the Morava River in Zlín district, Czech Republic. Chemosphere 151, 225–233.

Bonina, S.M.C., Codling, G., Corcoran, M.B., Guo, J., Giesy, J.P., Li, A., Sturchio, N.C., Rockne, K.J., 2018. Temporal and spatial differences in deposition of organic matter and black carbon in Lake Michigan sediments over the period 1850-2010. J. Great Lakes Res. 44, 705–715.

Bzdusek, P.A., 2005. PCB or PAH Sources and Degradation in Aquatic Sediments Determined by Positive Matrix Factorization. University of Wisconsin-Milwaukee. PhD thesis.

Bzdusek, P.A., Christensen, E.R., Lee, C.M., Pakdeesusuk, U., Freedman, D.L., 2006. PCB congeners and dechlorination in sediments of Lake Hartwell, South Carolina determined from cores collected in 1987 and 1998. Environ. Sci. Technol. 40, 109–119.

Cao, Y., Cao, X., Wang, H., Wan, Y., Wang, S., 2015. Assessment on the distribution and partitioning of perfluorinated compounds in the water and sediment of Nansi Lake, China. Environ. Monit. Assess. 187, 611.

Cao, D., Guo, J., Wang, Y., Li, Z., Liang, K., Corcoran, M.B., Hosseini, S., Bonina, S.M.C., Rockne, K.J., Sturchio, N.C., Giesy, J.P., Liu, J., Li, A., Jiang, G.B., 2017. Organophosphate esters in sediment of the Great lakes. Environ. Sci. Technol. 51, 1441–1449.

Codling, G., Vogt, A., Jones, P.D., Wang, T., Wang, P., Lu, Y.-L., Corcoran, M., Bonina, S., Li, A., Sturchio, N.C., Rockne, K.J., Ji, K., Khim, J.-S., Naile, J.E., Giesy, J.P., 2014. Historical trends of inorganic and organic fluorine in sediments of Lake Michigan. Chemosphere 114, 203–209.

Codling, G., Hosseini, S., Corcoran, M.B., Bonina, S., Lin, T., Li, A., Sturchio, N.C., Rockne, K.J., Ji, K., Peng, H., Giesy, J.P., 2018a. Current and historical concentrations of poly and perflurinated compounds in sediments of the northern Great Lakes – Superior, Huron, and Michigan. Environ. Pollut. 236, 373–381.

Codling, G., Sturchio, N.C., Rockne, K.J., Li, A., Peng, H., Tse, T.J., Jones, P.D., Giesy, J.P., 2018b. Spatial and temporal trends in poly-and per-fluorinated compounds in the laurentian Great lakes Erie, Ontario and St. Clair. Environ. Pollut. 237, 396–405.

Corcoran, M., Sherif, M.I., Smalley, C., Li, A., Rockne, K.J., Giesy, J.P., Sturchio, N.C., 2018. Accumulation rates, focusing factors, and chronologies from depth profiles of ^{210}Pb and ^{137}Cs in sediments of the Laurentian Great Lakes. J. Great Lakes Res. 44, 693–704.

ECHA, 2019. One New Substance Added to the Candidate List, Several Entries Updated. European Chemicals Agency. https://echa.europa.eu/-/one-new-substance-added-to-the-candidate-list. (Accessed 12 June 2019).

Fisher, J.B., Lick, W.J., McCall, P.L., Robbins, J.A., 1980. Vertical mixing of lake sediments by tubificid oligochaetes. J. Geophys. Res. Atmos. 85 (C7), 3997–4006.

Giesy, J.P., Kannan, K., 2001. Global distribution of perfluorooctane sulfonate in wildlife. Environ. Sci. Technol. 35, 1339–1342.

Giesy, J.P., Maburu, S.A., Martin, J.W., Kannan, K., Jones, P.D., Newsted, J.L., Coady, K., 2006. In: Hites, R.A. (Ed.), Perfluorinated Compounds in the Great Lakes. Persistent Organic Pollutants in the Great Lakes. Springer, Berlin Heidelberg, pp. 391–438.

Guo, J., Li, Z., Ranasinghe, P., Bonina, S., Hosseini, S., Corcoran, M.B., Smalley, C., Kaliappan, R., Wu, Y., Chen, D., Sandy, A.L., Wang, Y., Rockne, K.J., Sturchio, N.C., Giesy, J.P., Li, A., 2016. Occurrence of atrazine and related compounds in sediments of Upper Great Lakes. Environ. Sci. Technol. 50, 7335–7343.

Higgins, C.P., Luthy, R.G., 2006. Sorption of perfluorinated surfactants on sediments. Environ. Sci. Technol. 40, 7251–7256.

Hosseini, S., 2016. Implications of Carbon Deposition on the Fate of Semi-volatile Organic Pollutants in the Great Lakes. PhD. Dissertation. University of Illinois at Chicago.

Li, A., Rockne, K.J., Sturchio, N., Song, W., Ford, J.C., Buckley, D.R., Mills, W.J., 2006. Polybrominated diphenyl ethers in the sediments of the Great lakes. 4. Influencing factors, trends, and implications. Environ. Sci. Technol. 40, 7528–7534.

Li, A., Rockne, K.J., Sturchio, N., Song, W., Ford, J.C., Wei, H., 2009. PCBs in sediments of the Great Lakes - distribution and trends, homolog and chlorine patterns, and in situ degradation. Environ. Pollut. 157, 141–147.

Li, B., Ho, S.S.H., Xue, Y., Huang, Y., Wang, L., Cheng, Y., Dai, W., Zhong, H., Cao, J., Lee, S., 2017. Characterizations of volatile organic compounds at roadside environment: the first comprehensive study in Northwestern China. Atmos. Environ. 161, 1–12.

Li, A., Guo, J., Li, Z., Lin, T., Zhou, S., He, H., Ranansinghe, P., Sturchio, N.C., Rockne, K.J., Giesy, J.P., 2018. Legacy polychlorinated organic pollutants in the sediment of the Great Lakes. J. Great Lakes Res. 44, 682–692.

Loughran, D., Mangahas, S., 2019. PFOA & PFOS replacements under Fire. Praedicat. February 18. https://www.praedicat.com/pfoa-pfos-replacements-under-fire/. (Accessed 12 June 2019).

Myers, A.L., Crozier, P.W., Helm, P.A., Brimacombe, C., Furdui, V.I., Reiner, E.J., Burniston, D., Marvin, C.H., 2012. Fate, distribution, and contrasting temporal trends of perfluoroalkyl substances (PFASs) in Lake Ontario, Canada. Environ. Int. 44, 92–99.

Paatero, P., 1997. Least squares formulation of robust non-negative factor analysis.

Chemometr. Intell. Lab. Syst. 27, 23–35.
Paatero, P., Tapper, U., 1994. Positive matrix factorization: a nonnegative factor model with optimal utilization of error estimates of data values. Environmetrics 5, 111–126.
Praipipat, P., Rodenburg, P., L.A., Cavallo, G.J., 2013. Source apportionment of polychlorinated biphenyls in the sediments of the Delaware River. Environ. Sci. Technol. 47, 4277–4283.
Prevedouros, K., Cousins, I.T., Buck, R.C., Korzeniowski, S.H., 2006. Sources, fate and transport of perfluorocarboxylates. Environ. Sci. Technol. 40, 32–44.
Reemtsma, T., Berger, U., Arp, H.P.H., Gallard, H., Knepper, T.P., Neumann, M., Quintana, J.B., De Voogt, P., 2016. Mind the gap: persistent and mobile organic compounds – water contaminants that slip through. Environ. Sci. Technol. 50, 10308–10315.
Rodenburg, L.A., Meng, Q., Yee, D., Greenfield, B.K., 2014. Evidence for photochemical and microbial debromination of polybrominated diphenyl ether flame retardants in San Francisco Bay sediment. Chemosphere 106, 36–43.
Sundqvist, K.L., Tysklind, M., Geladi, P., Hopke, P.K., Wiberg, K., 2010. PCDD/F source apportionment in the Baltic Sea using positive matrix factorization. Environ. Sci. Technol. 44, 1690–1697.
US EPA, 2000. Perfluorooctyl Sulfonates; Proposed Significant New Use Rule. U.S. Environmental Protection Agency, pp. 62319–66233.
US EPA, 2013. Estimation program Interface (EPI) suite version 4.11. https://www.epa.gov/tsca-screening-tools/epi-suitetm-estimation-program-interface.
US EPA, 2018a. 2010/2015 PFOA Stewardship Program. United States Environmental Protection Agency.
US EPA, 2018b. PFAS what you need to know. https://www.epa.gov/sites/production/files/2018- 03/documents/pfasv15_2pg_0.pdf.
US EPA, 2018c. PFAS Research and Development. Community Engagement in Fayetteville, North Carolina. August 14, 2018,. https://www.epa.gov/sites/production/files/2018-08/documents/r4_combined_presentations_.pdf. (Accessed 14 June 2019).
Wang, Z., Cousins, I.T., Scheringer, M., Hungerbühler, K., 2013. Fluorinated alternatives to long-chain perfluoroalkyl carboxylic acids (PFCAs), perfluoroalkane sulfonic acids (PFSAs) and their potential precursors. Environ. Int. 60, 242–248.
Wang, Z., Cousins, I.T., Scheringer, M., Buck, R.C., Hungerbühler, K., 2014a. Global emission inventories for C_4-C_{14} perfluoroalkyl carboxylic acid (PFCA) homologues from 1951 to 2030, Part II: the remaining pieces of the puzzle. Environ. Int. 69, 166–176.
Wang, Z., Cousins, I.T., Scheringer, M., Buck, R.C., Hungerbühler, K., 2014b. Global emission inventories for C_4-C_{14} perfluoroalkyl carboxylic acid (PFCA) homologues from 1951 to 2030, Part I: production and emissions from quantifiable sources. Environ. Int. 70, 62–75.
Yang, R., Wei, H., Guo, J., McLeod, C., Li, A., Sturchio, N.C., 2011. Historically and currently used dechloranes in the sediments of the Great lakes. Environ. Sci. Technol. 45, 5156–5163.
Yang, R., Wei, H., Guo, J., Li, A., 2012. Emerging brominated flame retardants in the sediment of the Great lakes. Environ. Sci. Technol. 46, 3119–3126.
Yeung, L.W.Y., De Silva, A.O., Loi, E.I.H., Marvin, C.H., Taniyasu, S., Yamashita, N., Mabury, S.A., Muir, D.C.G., Lam, P.K.S., 2013. Perfluoroalkyl substances and extractable organic fluorine in surface sediments and cores from Lake Ontario. Environ. Int. 59, 389–397.
Zhao, L., Zhu, L., Yang, L., Liu, Z., Zhang, Y., 2012. Distribution and desorption of perfluorinated compounds in fractionated sediments. Chemosphere 88, 1390–1397.
Zou, Y., Aziz-Schwanbeck, A.C., Wei, H., Christensen, E.R., Rockne, K., Li, A., 2016. Debromination of PBDEs in Arkansas water bodies analyzed by positive matrix factorization. Environ. Sci. Technol. 50, 1359–1367.
Zushi, Y., Tamada, M., Kanai, Y., Masunaga, S., 2010. Time trends of perfluorinated compounds from the sediment core of Tokyo Bay, Japan (1950s-2004). Environ. Pollut. 158, 756–763.

Appendix A. Supplementary data

Poly- and per-fluoroalkyl compounds in sediments of the Laurentian Great Lakes: Loadings, temporal trends, and sources determined by positive matrix factorization

Erik R. Christensen[a,*], Ruijie Zhang[b,c], Garry Codling[d], John P. Giesy[e,f], An Li[b]

[a]Department of Civil and Environmental Engineering, University of Wisconsin-Milwaukee, Milwaukee, WI 53201, USA

[b] School of Public Health, University of Illinois at Chicago, Chicago, IL 60612, USA

[c] School of Marine Sciences, Guangxi University, Nanning 530004, China

[d]Research Centre for Contaminants in the Environment, Pavilion 29, Masaryk University, Brno, Czech Republic

[e]Department of Veterinary Biomedical Sciences and Toxicology Centre, University of Saskatchewan, Saskatoon, SK S7N 5B3, Canada

[f]Department of Environmental Science, Baylor University, Waco, TX, United States

*corresponding author's email: erc@uwm.edu

Table of Contents

(2 pages text and references, 8 Tables, 6 Figures)

PMF solution procedure and application to Lakes Erie and Ontario. The number of factors was determined such that the weighted sum of squares of differences between measured and calculated concentrations, Q, was about equal to the number of degrees of freedom, $df = m \times n - f \times (m + n)$. Q is calculated (Equation 1).

$$Q = \sum_{i=1}^{m} \sum_{j=1}^{n} \frac{(X_{ij} - \sum_{h=1}^{f} G_{ih} F_{hj})^2}{\sigma_{ij}^2} \quad (1)$$

where $i = 1, \ldots, m$, $j = 1, \ldots, n$, and $h = 1, \ldots, f$ indicate compounds, samples and factors, and σ_{ij} is the standard deviation of compound i in sample j. Other criteria for the number f of factors selected was that addition of another factor p+1 should maintain stability of the solution and include loading matrices determined by p factors. The loading and score matrices contained several zeros such that rotational ambiguity was negligible. The computer program for positive matrix factorization (PMF) was from the PhD thesis of Bzdusek (Bzdusek, 2005). Exner (< 0.1) and coefficients of determination for individual chemicals (>0.65) were considered for goodness of fit. Because of greater concentrations of PFASs in Lakes Erie and Ontario, compared with the other Great Lakes, the PMF modeling focused on Lakes Erie and Ontario. Note that Rockne et al. (2015) attempted to apply PMF to the Great Lakes sediment, however without success, stating that the reason for this was that PFAS levels in the Great Lakes were below detection limit for a high percentage of the samples.

For Lake Erie, all available cores ER09, ER15, ER37, ER73, and ER92 were considered. Of these cores, ER09 and ER92 were chosen to maximize segments with PFASs greater than the detection limit for PFOS, PFOA, PFHxA, PFDA, PFBS, PHHxS, PFDS, FOSA and PFUdA. Core ER92 is near the inflow and core ER09 near the outflow of Lake Erie (Codling et al., 2018). Eliminating all but PFOS, PFOA, PFHxA, PFDA, PFHxS, and PFUdA to keep measurable segments above 75%, did not produce a useable PMF solution. Leaving out further PFDA and PFUdA, the resulting 4 x 40 (No. of chemicals x No. of samples) matrix still did not produce an acceptable solution. Part of the reason for this might be the shallowness and known significant sediment mixing of Lake Erie (Fisher et al., 1980). Mixing may also be inferred from the near-constant total ^{210}Pb and ^{137}Cs depth profiles in the upper 6-21 cm of cores ER09 and ER92 (Corcoran et al., 2018).

A similar procedure was more successful for Lake Ontario when using all available cores ON02, ON06, ON13, ON17, ON25, ON30, and ON36. The final data matrix was 8 x 40 including cores ON02, ON36 and the PFASs PFOS, PFHxA, PFHpA, PFNA, PFDA, PFBS, PFHxS, PFTrDA with 87% measurable segments. Cores ON02 and ON36 were from the inflow and outflow of Lake Ontario respectively. PFUdA was first included with 90% measurable segments, but the coefficient of determination was not acceptable (<0.1), so PFUdA

was removed. An inspection of PFUdA concentrations for cores ON02 and ON36 revealed large variability, some of which might be due to restriction of production of PFUdA after the mid-1980s (Codling et al., 2018). For samples with concentrations that were less than the detection limit (DL), the concentration was replaced by values from a Monte Carlo Gaussian distribution with 0.2 variance centered around DL/2.

REFERENCES

Bzdusek, P.A. 2005. PCB or PAH Sources and Degradation in Aquatic Sediments determined by Positive Matrix Factorization. PhD thesis, University of Wisconsin-Milwaukee.

Codling, G., Sturchio, N.C., Rockne, K.J., Li, A.; Peng, H., Tse,T.J., Jones, P.D., Giesy, J.P. 2018. Spatial and temporal trends in poly-and per-fluorinated compounds in the Laurentian Great Lakes Erie, Ontario and St. Clair. Environ. Pollut. 237, 396-405.

Corcoran, M., Sherif, M.I., Smalley, C., Li, A., Rockne, K.J., Giesy, J.P., Sturchio, N.C. 2018. Accumulation rates, focusing factors, and chronologies from depth profiles of ^{210}Pb and ^{137}Cs in sediments of the Laurentian Great Lakes. J. Great Lakes Res. 44, 693-704.

Fisher, J.B., Lick, W.J., McCall, P.L., Robbins, J.A. 1980. Vertical mixing of lake sediments by tubificid oligochaetes. J. Geophys. Res. - Atmospheres 85, C7, 3997-4006.

Li, A., Guo, J., Li, Z., Lin, T., Zhou, S, He, H., Ranansinghe, P., Sturchio, N.C., Rockne, K.J., Giesy J.P. 2018. Legacy polychlorinated organic pollutants in the sediment of the Great Lakes. J. Great Lakes Res. 44, 682-692.

Rockne, K.J., Giesy, J.P., Codling, G. 2015. Applications of environmental forensics for chemicals of emerging concern. PACIFICHEM 2015, Session 19: Chemicals of emerging concern: a global perspective. Honolulu, Hawaii, December 15-20.

US EPA. 2013. Estimation Program Interface (EPI) Suite version 4.11 https://www.epa.gov/tsca-screening-tools/epi-suitetm-estimation-program-interface

US NIH. 2019. PubChem, National Library of Medicine, National Center for Biotechnology Information. https://pubchem.ncbi.nlm.nih.gov/compound/Perfluorooctane-sulfonic-acid#section=Octanol-Water-Partition-Coefficient

Table S1. Three sites with greatest concentrations of Σ_{22}PFASs.

Water Body	Based on concentration in Ponar grabs			Based on inventories in cores		
	#1	#2	#3	#1	#2	#3
Lake Superior	S119 Ontonagon	S104 Marathon - Wawa	S022 Superior/ Duluth	S001 Entrance to North Channel	S002 Wawa -North Channel	S019 Duluth
Lake Michigan	M116 Inlet to Lake Huron	M050 Green Bay	M120 Green Bay – Lake Huron	M041 Sturgeon Bay - Frankfort	M008 Southern Basin	M009 South Haven
Lake Huron	H108 Alpena - Saginaw	H048 Alpena – Georgian Bay	H118 Alpena	H048 Alpena – Georgian Bay	H032 Southern Basin	H006 Bluewater - Sarnia
North Channel/ Georgian Bay	GB39 Manitoulin Island - French River	NC82 Shesheg-waning	NC70 Meldrum Bay			
Lake Erie	ER38 Chatham - Kent	ER21 Detroit River Mouth	ER60 Detroit River Mouth	ER92 Leamington	ER15 Old Cut	ER09 Buffalo - Outlet
Lake Ontario	ON14 Cobourg	ON12 Lyndonville	ON16 Mid-lake	ON06 Niagara River Mouth	ON36 Wolfe Island Outlet	ON02 Niagara River Mouth - Hamilton
All Lakes	ON14	ON12	ER38	ER92	ON06	ON36

Table S2. Lake-wide recent annual loading of individual PFAS in sediments of the Great Lakes (kg/y).

Compound	Superior	Michigan	Huron	Erie	Ontario	All Lakes
Perfluoroalkyl compounds						
PFBA	2.2	1.2	16.6	50.9	48.9	119.8
PFPeA	2.4	0.9	25.0	63.0	3.6	94.9
PFHxA	1.1	2.5	7.4	28.2	22.1	61.3
PFHpA	3.9	9.6	3.6	1.6	2.2	20.8
PFOA	7.0	13.5	12.3	6.6	41.1	80.5
PFNA	6.5	6.6	6.6	9.4	53.6	82.7
PFDA	9.2	9.7	0.2	29.1	73.8	122.0
PFUnDA	5.6	2.2	8.3	378.2	42.2	436.5
PFDoDA	0	0.5	3.5	0	0.4	4.5
PFTrDA	9.5	0.3	0.2	3.9	82.6	96.6
PFTeDA	9.3	0.4	0.3	3.8	45.1	58.9
PFHxDA	0.0	0.5	0.1	0	4.0	4.6
PFBS	5.8	1.0	0.6	146.3	97.7	251.3
PFHxS	0	2.3	3.1	4.7	10.1	20.3
PFOS	4.5	52.8	20.5	44.1	130.5	252.5
PFDS	24.2	1.6	0.2	27.7	24.1	77.7
Perfluorinated precursors						
FOSA	0	0.1	0	3.8	0	3.9
FOSAA	1.2	1.1	0.4	[b]0	1.4	4.1
N-MeFOSAA	5.0	0.9	[a]na	5.4	0	11.3
NEtFOSAA	0.4	0.9	na	1.9	1.1	4.2
NMeFOSE	0	2.0	na	na	na	2.0
NEtFOSE	0	2.0	na	Na	na	2.0
∑PFASs	98 ± 27	113 ± 22	109 ± 31	809 ± 282	684 ± 145	1812 ± 320

[A]na = not analyzed; [b]0 = not detected

Table S3. Summary of regression analyses for concentrations of ∑22 PFASs

N	Intercept	a	b	R^2	*F*	*p-level*
	Ln Concentration (ng/g dw) = intercept + a × Latitude + b × Longitude					
166	26.78 ± 2.02	-0.315 ± 0.046	0.137 ± 0.023	0.489	78.03	1.68E-24
	Ln Concentration (ng/g OC) = intercept + a × Latitude + b × Longitude					
166	24.97 ± 2.86	-0.192 ± 0.065	0.128 ± 0.033	0.217	22.61	2.16E-09
	Ln Concentration (ng/g OC) = intercept + a × Latitude + b × Longitude					
[a]96	21.67 ± 2.65	-0.260 ± 0.066	0.057 ± 0031	0.290	18.99	1.22E-07
	Ln Inventory (ng/cm^2) = intercept + a × Latitude + b × Longitude					
40	24.65 ± 4.95	-0.153 ± 0.120	0.166 ± 0.057	0.343	9.68	4.15E-04

[a]Depositional locations only

Table S4. Estimation of Doubling Time (t_2). *

Site	N	∑22PFASs				PFOS			
		R^2	SLOPE	P	t_2, yr	R^2	SLOPE	p	t_2, yr
S002	3	0.768	0.013	0.320	55				
S008	5	0.273	0.020	0.366	35				
S011	7	0.443	0.014	0.103	50	**0.594**	**0.020**	**0.042**	**35**
S012	5	0.006	-0.001	0.904	-629	1.000	-0.058		-12
S016	5	0.744	0.035	0.060	20	0.445	0.025	0.219	28
S019	6	0.303	0.018	0.258	40	0.485	-0.033	0.124	-21
S022	11	**0.540**	**-0.027**	**0.010**	**-26**	0.106	-0.009	0.328	-75
M008	7	**0.812**	**0.027**	**0.006**	**26**	**0.804**	**0.027**	**0.006**	**26**
M009	12	0.207	0.010	0.138	68	**0.769**	**0.037**	**0.000**	**19**
M011	11	**0.890**	**0.030**	**0.000**	**23**	**0.906**	**0.029**	**0.000**	**24**
M018	6	**0.820**	**0.045**	**0.013**	**15**	**0.836**	**0.041**	**0.011**	**17**
M024	8	**0.829**	**0.023**	**0.002**	**30**	**0.806**	**0.022**	**0.002**	**32**
M032	8	**0.605**	**0.026**	**0.023**	**26**	**0.557**	**0.021**	**0.034**	**32**
M041	9	0.130	0.013	0.340	53	**0.849**	**0.045**	**0.000**	**15**
M047	10	**0.571**	**0.017**	**0.011**	**41**	**0.905**	**0.033**	**0.000**	**21**
M050	12	**0.755**	**0.034**	**0.000**	**20**	**0.833**	**0.051**	**0.000**	**14**
H001	15	0.059	0.017	0.381	40	0.052	0.008	0.412	88
H006	8	0.368	0.015	0.111	45	**0.631**	**0.020**	**0.018**	**36**
H012	11	0.241	0.055	0.125	12	0.226	0.048	0.139	14
H032	12	0.223	0.019	0.121	37	**0.582**	**0.052**	**0.004**	**13**
H038	6	0.356	-0.021	0.211	-34				
H048	5	0.146	0.010	0.525	72	**0.892**	**0.033**	**0.015**	**21**
H061	4	0.826	0.024	0.091	29	0.826	0.023	0.091	30
H095	5	0.247	0.024	0.394	29	0.008	0.002	0.883	348
ER09	20	0.166	0.040	0.075	17	0.008	-0.011	0.711	-65
ER15	20	0.055	0.025	0.319	28	0.002	0.002	0.843	458
ER37	19	**0.745**	**0.034**	**0.000**	**20**	0.035	0.003	0.446	220
ER73	20	0.002	0.003	0.865	227	0.001	0.001	0.881	558
ER92	16	**0.384**	**-0.029**	**0.011**	**-24**	**0.358**	**0.013**	**0.014**	**52**
ON02	7	0.447	0.017	0.101	42	**0.915**	**0.063**	**0.001**	**11**
ON06	20	**0.509**	**0.056**	**0.000**	**12**	0.195	0.042	0.051	16
ON13	8	**0.930**	**0.046**	**0.000**	**15**	**0.918**	**0.069**	**0.000**	**10**
ON17	11	0.079	0.017	0.404	42	0.082	0.019	0.392	37
ON25	10	**0.511**	**0.052**	**0.020**	**13**	**0.833**	**0.062**	**0.000**	**11**
ON30	11	**0.401**	**0.024**	**0.036**	**29**	**0.778**	**0.058**	**0.000**	**12**
ON36	11	0.093	0.007	0.361	96	**0.540**	**0.013**	**0.010**	**54**

* Linear regression Ln Flux vs. deposition year, using data after year 1940. Bold means statistically significant at 95% confidence level, and red indicates declining with $t_{1/2}$.

Table S5 Data matrix (ng/g dw) for 8 PFASs in 40 core samples from cores ON02 and ON36.

	PFOS	PFHxA	PFHpA	PFNA	PFDA	PFBS	PFHxS	PFTrDA
Detection limit	0.053	0.055	0.019	0.033	0.049	0.307	0.063	0.078
ON02MC-01	20.305	5.563	0.077	0.053	3.229	8.045	0.909	0.399
ON02MC-02	12.444	5.562	0.146	3.268	2.799	5.120	0.399	0.256
ON02MC-03	20.751	0.511	0.123	1.205	1.840	8.158	0.276	0.344
ON02MC-04	6.022	0.397	0.032	0.472	0.728	12.055	0.293	0.368
ON02MC-05	1.489	0.402	0.034	0.218	2.822	15.805	1.422	0.031
ON02MC-06	0.785	1.628	[a]0.010	0.014	10.212	8.674	2.914	0.033
ON02MC-07	0.529	1.044	0.010	0.494	1.229	5.174	2.846	0.042
ON02MC-08	0.337	0.548	0.008	0.176	0.432	9.358	0.341	0.041
ON02MC-09	0.899	0.798	0.013	0.176	0.093	4.289	0.117	0.138
ON02MC-10	0.485	0.515	0.065	0.018	0.278	8.951	0.050	0.045
ON02MC-11	0.321	0.300	0.032	0.171	0.013	10.846	0.576	0.165
ON02MC-12	2.670	1.103	0.037	0.284	1.127	11.842	0.728	0.045
ON02MC-13	0.091	0.473	0.007	0.139	0.022	14.123	0.406	0.091
ON02MC-14	0.069	0.804	0.011	0.019	0.835	18.440	0.658	0.035
ON02MC-15	0.293	0.637	0.006	0.055	0.031	10.362	0.273	0.084
ON02MC-16	2.426	0.853	0.085	0.340	1.660	22.313	0.264	0.035
ON02MC-17	0.516	1.679	0.006	0.016	0.034	5.653	1.266	0.034
ON02MC-18	0.084	0.264	0.008	0.137	0.133	12.082	0.153	0.094
ON02MC-19	0.255	0.383	0.045	0.115	0.097	17.785	0.027	0.108
ON02MC-20	0.621	1.958	0.081	0.016	0.025	15.416	0.956	0.033
ON36MC-01	6.501	3.762	0.190	2.336	3.086	12.461	2.915	1.881
ON36MC-02	6.728	3.806	0.199	2.644	2.489	19.452	3.628	3.433
ON36MC-03	3.240	1.546	0.125	0.865	1.515	7.384	2.815	0.941
ON36MC-04	7.304	6.381	0.246	3.503	3.923	16.751	4.598	3.567
ON36MC-05	3.888	8.434	0.215	2.363	4.938	16.812	3.058	4.132
ON36MC-06	3.876	1.107	0.115	2.419	2.808	0.018	3.144	3.285
ON36MC-07	3.344	7.308	0.155	5.324	2.937	20.941	1.678	3.554
ON36MC-08	4.245	0.057	0.187	3.995	3.491	77.823	3.369	2.947
ON36MC-09	2.193	7.094	0.153	3.262	2.815	20.134	4.202	2.533
ON36MC-10	3.451	1.946	0.188	3.190	1.629	9.293	6.912	1.129
ON36MC-11	2.683	11.486	0.150	3.780	3.025	14.407	3.272	2.311
ON36MC-12	2.409	9.718	0.153	3.016	4.271	17.800	5.124	6.362
ON36MC-13	2.793	3.571	0.274	4.799	3.643	8.441	6.276	2.271
ON36MC-14	0.026	0.239	0.064	0.015	0.027	0.130	0.659	0.031
ON36MC-15	3.175	4.969	0.199	4.624	4.009	8.680	6.805	2.640
ON36MC-16	2.482	11.358	0.214	5.075	4.185	17.918	5.501	3.876
ON36MC-17	2.373	7.636	0.283	4.225	4.776	16.912	5.646	2.721
ON36MC-18	2.307	3.596	0.394	4.206	9.254	16.126	8.120	4.521
ON36MC-19	8.177	0.027	0.428	0.021	0.020	0.160	0.028	0.041
ON36MC-20	2.011	7.151	0.274	3.328	3.681	11.036	5.141	4.024

[a]Below detection limit in red

Table S6. Calculated Log K_{oc} values for PFASs considered in PMF model.

Compound	Structural formula	MW	pKa[a]	Log K_{oc}[b]
PFHxA	$C_6HF_{11}O_2$	314.1	-0.16	2.08
PFHpA	$C_7HF_{13}O_2$	364.1	-2.29	2.45
PFNA	$C_9HF_{17}O_2$	464.1	-0.21	3.19
PFDA	$C_{10}HF_{19}O_2$	514.1	--	3.56
PFTrDA	$C_{13}HF_{25}O_2$	664.1	--	4.67
PFBS	$C_4F_9SO_3H$	300.1	-3.31	1.93
PFHxS	$C_6HF_{13}O_3S$	400.1	0.14	2.67
PFOS	$C_8F_{17}SO_3H$	500.1	< 1.0	3.41

[a]From US NIH PubChem data base (2019). [b]Calculated by use of the EPI Suite K_{ow} method (US EPA 2013). Note that K_{oc} is sensitive to pH. The listed K_{oc} -values represent a best-fit to most experimental values at ambient pH for each compound, corresponding to full ionization of the compounds.

Table S7. Fractions of eight PFASs, considered in PMF modeling with calculated K_{oc} values, in pore water for Lake Ontario core ON02.

Core	Depth	ρ_b[a]	Φ[b]	r_{sw}[c]	f_{oc}[d]	f_{iw}[e]							
Section	cm	g/cm^3	%		mg/g	PFOS	PFBS	PFHxS	PFHxA	PFHpA	PFNA	PFDA	PFTrDA
ON02-01	0-1	0.10	96	0.10	49.4	0.070	0.70	0.29	0.62	0.41	0.111	0.051	0.0041
ON02-02	1-2	0.15	94	0.16	43.8	0.051	0.62	0.23	0.54	0.33	0.082	0.037	0.0030
ON02-03	2-3	0.17	93	0.18	43.8	0.046	0.59	0.21	0.51	0.31	0.074	0.033	0.0027
ON02-04	3-4	0.19	92	0.21	49.7	0.036	0.53	0.17	0.45	0.26	0.059	0.026	0.0021
ON02-05	4-5	0.21	92	0.23	46.9	0.035	0.52	0.16	0.43	0.25	0.056	0.025	0.0020
ON02-06	5-6	0.25	90	0.27	35.9	0.038	0.54	0.18	0.46	0.27	0.062	0.027	0.0022
ON02-07	6-7	0.32	87	0.37	26.9	0.038	0.54	0.18	0.46	0.26	0.061	0.027	0.0022
ON02-08	7-8	0.37	86	0.43	18.5	0.047	0.60	0.21	0.51	0.31	0.075	0.033	0.0027
ON02-09	8-9	0.39	85	0.45	17.2	0.048	0.60	0.22	0.52	0.31	0.076	0.034	0.0027
ON02-10	9-10	0.37	86	0.43	17.1	0.050	0.62	0.23	0.53	0.33	0.081	0.036	0.0029
ON02-11	10-12	0.37	85	0.44	16.1	0.052	0.62	0.23	0.54	0.33	0.084	0.038	0.0030
ON02-12	12-14	0.35	86	0.41	17.0	0.053	0.63	0.23	0.54	0.34	0.085	0.038	0.0031
ON02-13	14-16	0.36	86	0.41	17.3	0.052	0.62	0.23	0.54	0.33	0.083	0.037	0.0030
ON02-14	16-18	0.37	86	0.43	17.1	0.050	0.61	0.23	0.53	0.33	0.081	0.036	0.0029
ON02-15	18-20	0.38	85	0.44	16.5	0.051	0.62	0.23	0.53	0.33	0.081	0.036	0.0029
ON02-16	20-22	0.39	85	0.46	15.4	0.052	0.62	0.23	0.54	0.33	0.083	0.037	0.0030
ON02-17	22-24	0.38	85	0.45	16.0	0.051	0.62	0.23	0.54	0.33	0.082	0.037	0.0030
ON02-18	24-26	0.38	85	0.44	16.0	0.052	0.62	0.23	0.54	0.33	0.083	0.037	0.0030
ON02-19	26-28	0.38	85	0.45	15.5	0.053	0.63	0.24	0.54	0.34	0.085	0.038	0.0031
ON02-20	28-30	0.39	85	0.46	15.5	0.051	0.62	0.23	0.54	0.33	0.082	0.037	0.0030

[a]ρ_b = dry bulk density, [b]φ = porosity, [c]r_{sw} = solid-to-water mass ratio, [d]f_{oc} = organic carbon fraction, [e]f_{iw} = fraction in interstitial (pore) water

Table S8. Fractions of eight PFASs, considered in PMF modeling with calculated K_{oc} values, in pore water for Lake Ontario core ON36.

Core	Depth	ρ_b[a]	Φ[b]	r_{sw}[c]	f_{oc}[d]	f_{iw}[e]							
Section	cm	g/cm^3	%		mg/g	PFOS	PFBS	PFHxS	PFHxA	PFHpA	PFNA	PFDA	PFTrDA
ON36-01	0-1	0.12	95	0.12	70.6	0.043	0.57	0.20	0.49	0.29	0.069	0.030	0.0024
ON36-02	1-2	0.16	93	0.17	64.2	0.034	0.51	0.16	0.43	0.24	0.054	0.024	0.0019
ON36-03	2-3	0.20	92	0.22	59.5	0.029	0.47	0.14	0.39	0.21	0.047	0.021	0.0016
ON36-04	3-4	0.23	91	0.25	58.0	0.026	0.44	0.13	0.36	0.19	0.042	0.018	0.0015
ON36-05	4-5	0.22	91	0.24	56.5	0.027	0.46	0.13	0.38	0.20	0.045	0.020	0.0015
ON36-06	5-6	0.22	91	0.24	54.9	0.028	0.47	0.14	0.38	0.21	0.046	0.020	0.0016
ON36-07	6-7	0.22	91	0.24	54.2	0.029	0.47	0.14	0.39	0.21	0.047	0.021	0.0016
ON36-08	7-8	0.22	91	0.24	59.9	0.027	0.45	0.13	0.37	0.20	0.044	0.019	0.0015
ON36-09	8-9	0.22	91	0.24	56.0	0.028	0.46	0.14	0.38	0.21	0.045	0.020	0.0016
ON36-10	9-10	0.22	91	0.24	52.6	0.029	0.48	0.14	0.39	0.22	0.048	0.021	0.0017
ON36-11	10-12	0.23	91	0.26	51.9	0.028	0.47	0.14	0.38	0.21	0.046	0.020	0.0016
ON36-12	12-14	0.26	90	0.28	44.1	0.030	0.48	0.15	0.40	0.22	0.049	0.021	0.0017
ON36-13	14-16	0.30	88	0.34	45.3	0.025	0.44	0.12	0.35	0.19	0.041	0.018	0.0014
ON36-14	16-18	0.33	87	0.38	38.4	0.026	0.45	0.13	0.36	0.20	0.043	0.019	0.0015
ON36-15	18-20	0.33	87	0.38	36.3	0.028	0.46	0.13	0.38	0.21	0.045	0.020	0.0016
ON36-16	20-22	0.33	87	0.38	36.5	0.027	0.46	0.13	0.37	0.20	0.044	0.019	0.0015
ON36-17	22-24	0.32	88	0.36	31.5	0.033	0.51	0.16	0.42	0.24	0.054	0.024	0.0019
ON36-18	24-26	0.32	88	0.36	29.5	0.035	0.52	0.17	0.44	0.25	0.057	0.025	0.0020
ON36-19	26-28	0.31	88	0.35	27.4	0.039	0.55	0.18	0.46	0.27	0.063	0.028	0.0022
ON36-20	28-30	0.32	88	0.36	26.6	0.039	0.55	0.18	0.46	0.27	0.063	0.028	0.0022

[a]ρ_b = dry bulk density, [b]φ = porosity, [c]r_{sw} = solid-to-water mass ratio, [d]f_{oc} = organic carbon fraction, [e]f_{iw} = fraction in interstitial (pore) water

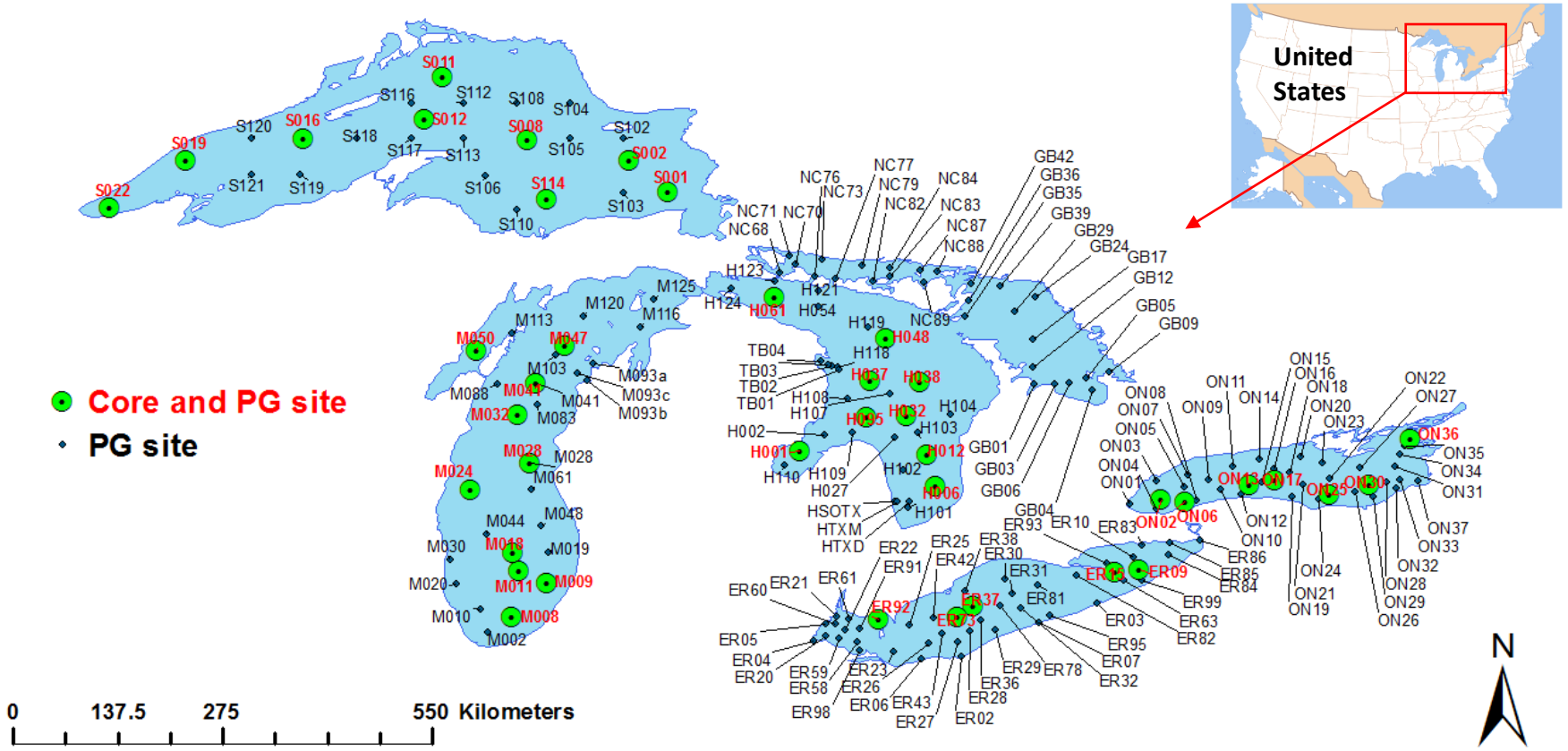

Figure S1. Sampling sites of sediment in the Great Lakes. Core and PG represent core and Ponar grab sediment, respectively. Ponar grab samples were also collected at all coring sites. This map was adopted from Li et al. (Li et al., 2018).

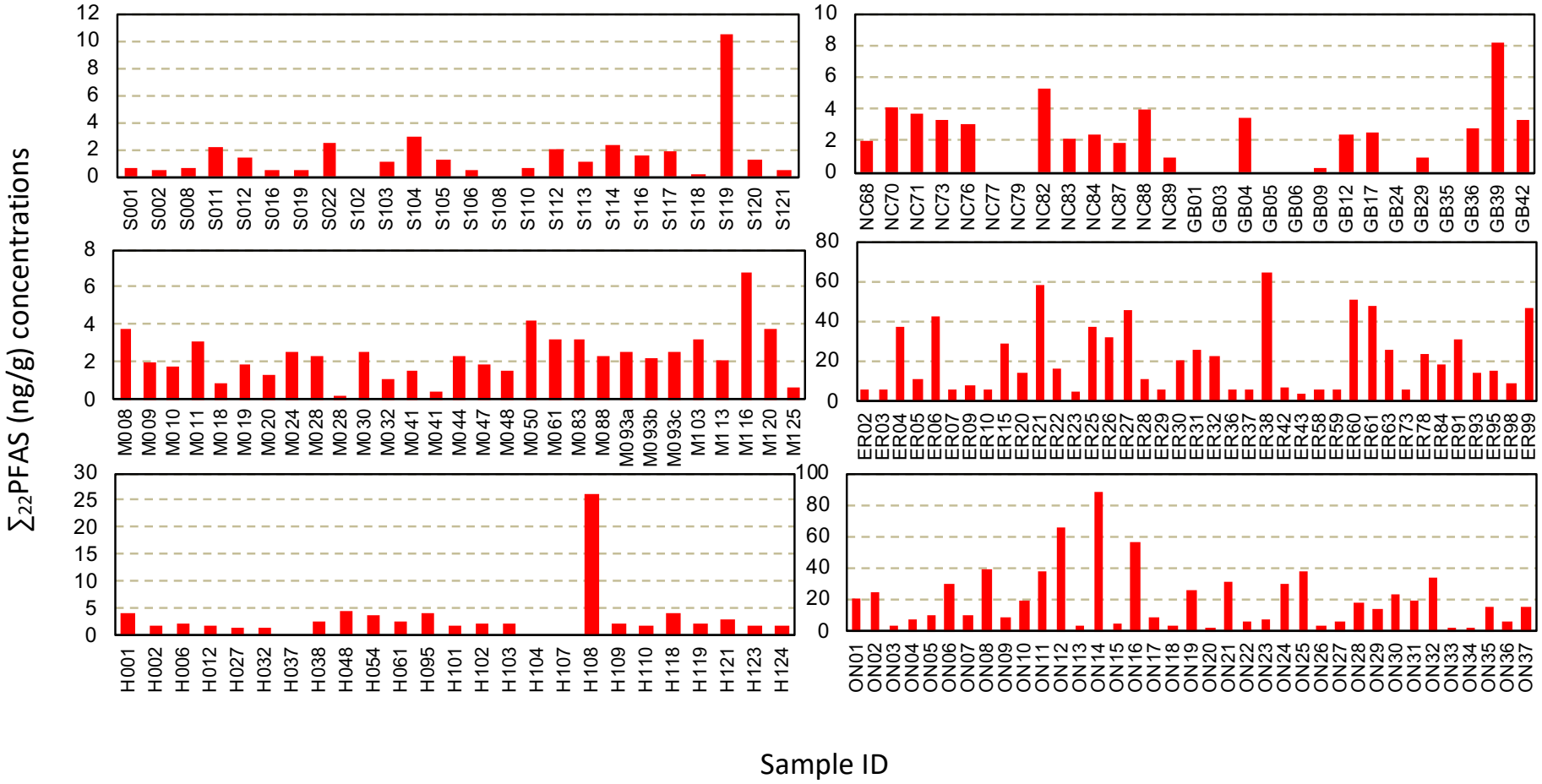

Figure S2. Concentrations (ng/g dw) in Ponar grab sediment samples.

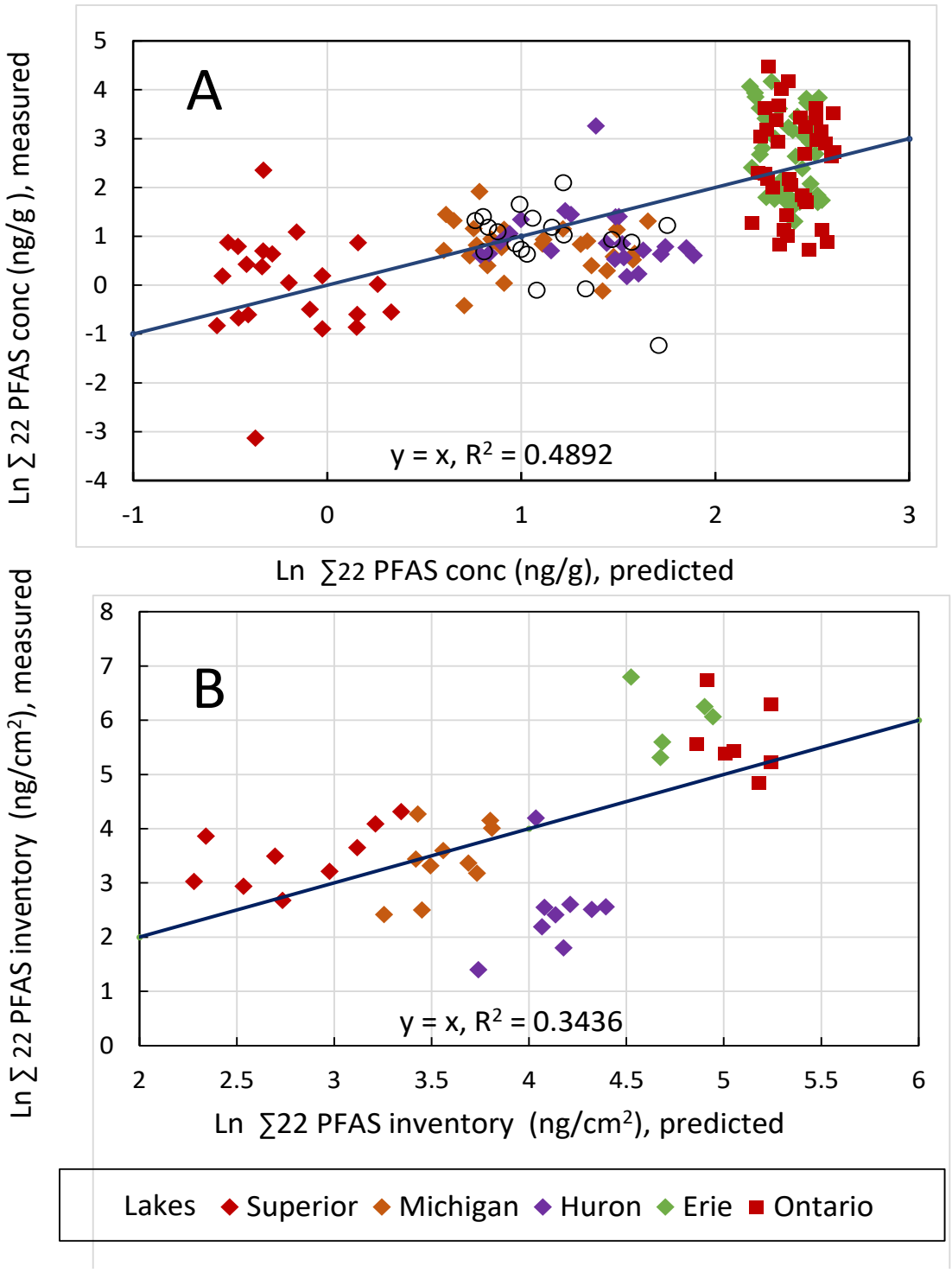

Figure S3. Comparison of predicted with measured (A) concentrations in Ponar grab samples and (B) inventories at coring sites, for $\sum_{22}$PFASs using multivariate linear regression models with latitude and longitude of sampling sites as independent variables. Open circles in A indicate the North Channel and Georgian Bay locations.

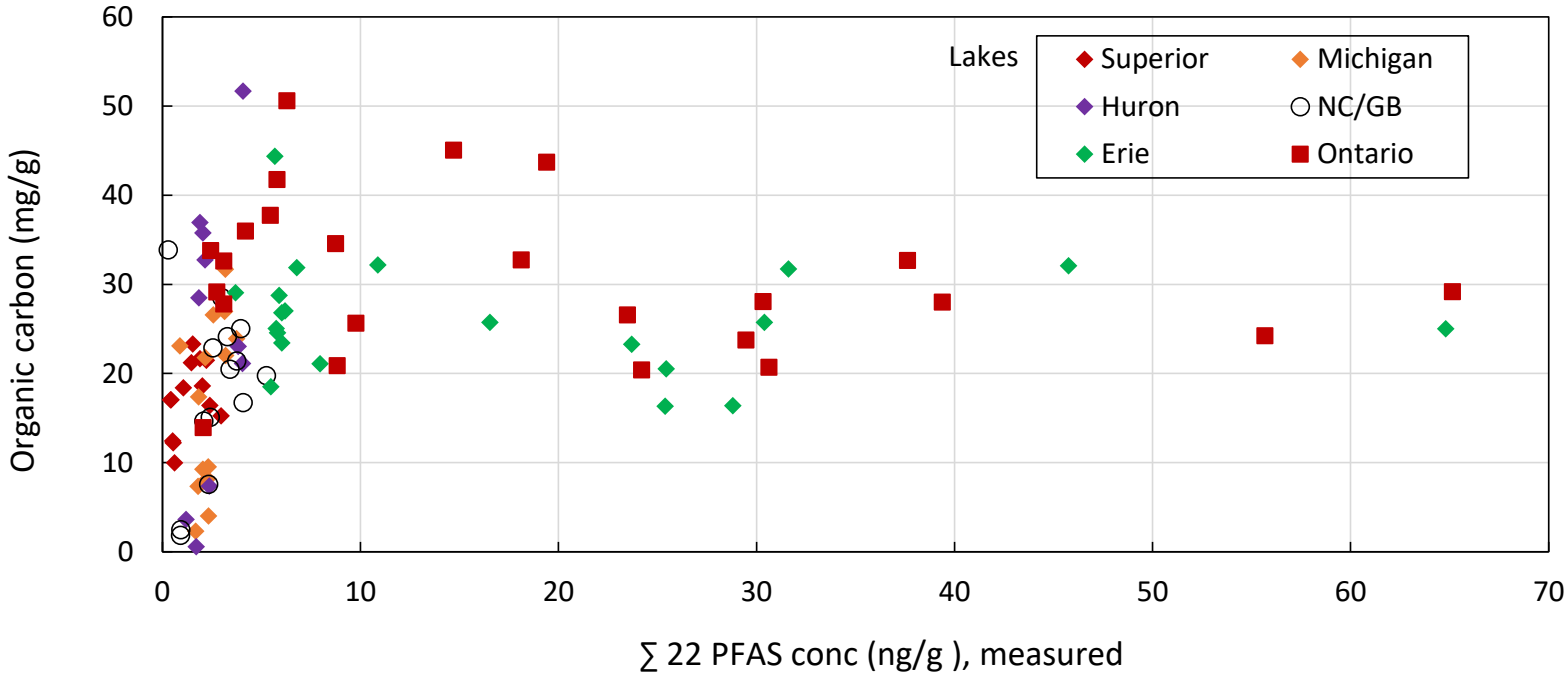

Fig. S4. Organic carbon (mg/g) vs $\sum_{22}$PFAS (ng/g) concentrations in Ponar grab samples. All samples with dry bulk density $\rho_b \leq 0.45$ g/cm^3 are shown, except an outlier from Lake Superior at S119 with $\sum_{22}$PFAS (ng/g) = 10.5 ng/g and OC = 16.29 mg/g.

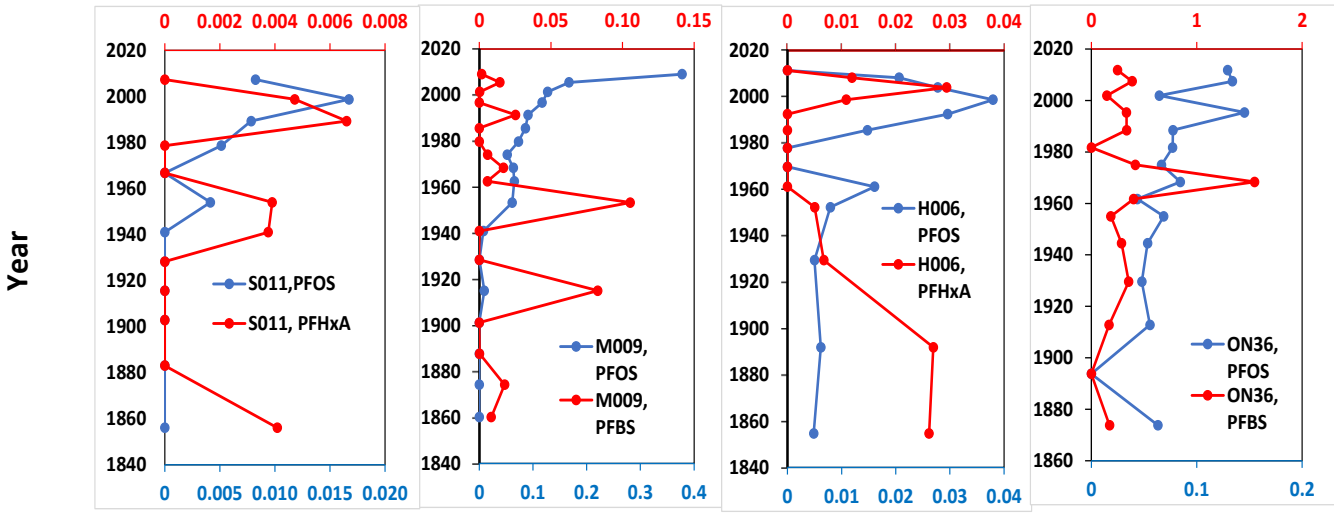

Core	Mass sedimentation rate (g/cm^2/yr)	FF
S011	0.01522	2.45
M009	0.065	2.20
H006	0.0323 (2011-1952)	2.17
ON36	0.033	1.65

Figure S5. Temporal trends of net fluxes in cores from Lakes Superior (S), Michigan (M), Huron (H), and Ontario (ON) of PFOS, which is mainly particle associated, and PFHxA or PFBS which both have significant fractions in porewater.

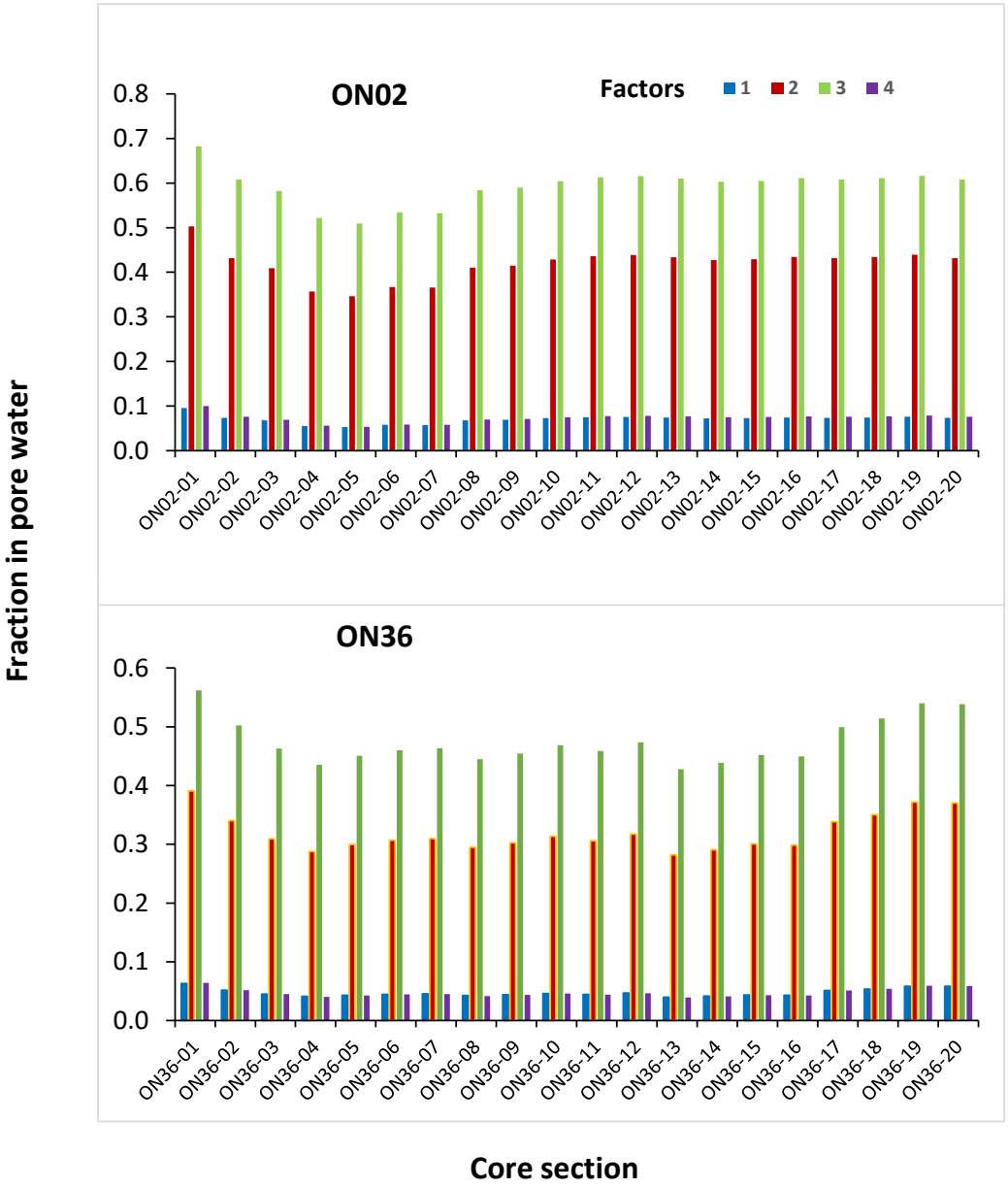

Figure S6. Calculated PFAS mass fractions in pore water of factors 1-4 in Ontario cores ON02 and ON36.